Solution of Viscous Flow around a Circular Cylinder by a New Integral Representation Method (NIRM)

H. Isshiki*, S. Nagata and Y. Imai

Institute of Ocean Enery , Saga University, Saga, Japan
*Email: isshiki {at} dab.hi-ho.ne.jp

ABSTRACT— ***New nonlinear integral representations (NIRM) are derived from a nonlinear differential-type boundary value problem using a fundamental solution of the primary space-differential operator of the differential equation. Integral representations are equivalent to differential equations. A set of integral representations is an integral-type boundary value problem. Unknown variables of a boundary value problem can be determined by solving a set of integral equations obtained from a set of integral representations. In the present paper, a set of integral representations using the fundamental solution of the primary space-differential operator is derived for viscous flows. The velocity, vorticity, and pressure of the Navier-Stokes equation can be determined by solving a set of integral equations obtained from a set of integral representations. A new numerical solution of the Navier-Stokes equation is proposed based on integral representations. The integral representation method was used to obtain the numerical results of low-Reynolds-number laminar flows around a circular cylinder. The narrower regions and coarser meshes are used in the numerical calculations using the integral representation method than in those using the ordinary FEM. The numerical results correctly reflect the experimental ones. Unlike FEM, as seen from that constant distribution of the unknown variables is possible, NIRM may not assume the continuity of the unknown variables between elements from the beginning. It would be safe to say this is a big advantage of NIRM.***

Keywords— New integral representation method (NIRM), Primary space-differential operator, Vorticity, Navier-Stokes equation

1. INTRODUCTION

Generally speaking, a physical phenomenon is described as a boundary value problem in differential equations, which may be referred to as a differential-type boundary value problem. Using a fundamental solution of the differential equations, we can derive integral representations from the differential-type boundary value problem. If we substitute the boundary condition into the integral representations, we obtain the integral equations. We can determine the unknown variables by solving the integral equations. Namely, the integral representations are equivalent to the differential equations. As such, we may refer to the boundary value problem expressed by the integral representations as an integral-type boundary value problem.

A solution using integral representations is widely used in potential flow calculations as the boundary element method. In the case of viscous flow calculations, Wu conducted a series of studies [1-4] and verified the effectiveness of the method through numerical calculations. However, according to his principal idea, although he used integral representations to obtain the velocity field from the vorticity field, he used differential equations to express the convective diffusion of the vorticity. He also proposed integral representations describing the convective diffusion of the vorticity, but these representations are different from those used in the present paper and were derived using a fundamental solution for the initial value problem. On the other hand, Uhlman obtained integral representations not only for the kinematic relations between the velocity and vorticity but also for the convective diffusion of the vorticity [5]. He pointed out the possibility of an integral-type boundary value problem, but did not mention how to apply his theory to computations and did not verify his theory through numerical calculations.

In the present paper, we discuss the integral-type boundary value problems from a similar viewpoint as Uhlman and propose a new numerical method for solving the Navier-Stokes equation. The proposed method has the following characteristics:

(1) Although the vorticity is the most important variables, the proposed method differs from the vortex particle method [6] in that the vorticity distribution is treated as that of particles. Although appropriate for treating the convection, the vortex particle method can't treat the viscous diffusion precisely. The vortex particle method is mathematically correct for non-viscous fluid. However, in case of viscous flow, the introduction of viscous diffusion of

vortex blob is not mathematically strict. It's a kind of heuristic approach. Hence, it can't give a mathematically correct way to increase the accuracy of the viscous diffusion effect. However, the authors admit that the vortex particle method is one of the practical methods and is very useful in many practical problems. The proposed method treats the diffusion as well as convection correctly, and as such may be suitable for discussing diffusion-dominant problems.

(2) The present method is a unique numerical method that is based on integral representations of the velocity, vorticity, and pressure reported by Uhlman [5].

(3) Uhlman's integral representations do not include differentiations of unknown variables by space variables. Since the differential operations by space variables are replaced by integral operations, we can easily introduce an irregular element division of the space. The proposed method would be favorable for cases in which the fluid region is geometrically complex and/or the boundary changes in time and the element division becomes irregular. If the boundary does not change in time, we are not required to obtain the inverse of the matrices at every step. Since the inverse is required to be obtained once at the beginning of the calculation, the load of the calculation would not increase significantly.

(4) Since we need to consider only the region in which the vorticity exists, the required calculation time and computer memory are reduced.

For the understanding of the readers, we add the following descriptions. Reference [12-15] were added as the results of survey on recent developments with respect to integral equation method (IEM), or integral representation method (IRM), on unsteady Navier-Stokes equation (UNSE). These are boundary element method (BEM) or boundary integral method (BIM). It was not possible to find those about the idea of Uhlman by Uhlman or others. As the Solution of UNSE, there are time-space separate method (TSS) that handles time and space in different way and time-space unified method (TSU) that treats time and space as a unit. Finite difference method (FDM) is TSU, and Finite Element Method (FEM) is generally TSS, using difference equation (DE) in time and variational equation (VE) in space. This paper follows the TSS, and we use DE in time and IRM in space. As the fundamental solution, we use that of an appropriate space-differential operator. We use that of Laplace operator in this paper. If we use TSU, we use IRM in unified space including time.In this case, it is possible to derive the BIM [12-14]. A fundamental solution of an appropriate time-space-differential operator, for example, that of the linear unsteady diffusion problem is used. There is also a method that IRM is obtained for a part of the unknown variables, and the other variables are dealt with DE. For example, the relationship between vorticity and velocity is rewritten in the form of IRM, the so-called Biot-Savart law, and DE is used to deal with the time evolution of the vorticity. In this paper, IRM covers also time evolution of the vorticity.

In addition, the handling of nonlinear term is important in the solution of UNSE. If we treat the time evolution explicitly, it is simple because it does not require the iteration calculation. However, we have to reduce the time step. If we use implicit method, the iteration is required, but the time step can be greatly increased. From the viewpoint of the stability and accuracy, implicit solution is much better.

Reference [12] derives BIM for a steady solution of the Navier-Stokes equation. Fundamental solution of Stokes equation is applied there. Since It gave the direction of a new development in IEM, this idea should be appreciated highly. Although the idea of this paper is based on Uhlman's paper, Uhlman himself has not developed a numerical method specifically. The uniqueness of Uhlman's theory is that IRM derived by Uhlman with respect to the space portion of the unsteady differential equations for the vorticity does not include the spatial derivatives of the unknown variables. This paper is intended as well to complete the theory Uhlman, were subjected to numerical concrete. I'm dealing with the explicit development time.

In the present paper, we discuss the laminar flow alone and do not address the turbulent flow, but we will deal with the turbulent flow as the next step. As for the turbulent flow, we think the idea of this paper is valid in a significant portion. First, in order to increase the stability, accuracy and computational efficiency, we will introduce the implicit method for time-marching. Further, in order to increase the accuracy, we use currently the constant distribution of the unknown variables in elements, but should use the higher distribution. Unlike FEM, as seen from that constant distribution of the unknown variables is possible, IRM may not assume the continuity of the unknown variables between elements from the beginning. It would be safe to say this is a big advantage of IRM. On the preparation mentioned above, we intend to introduce a large eddy simulation.

2. BASIC EQUATIONS OF FLUID MOTION

We assume that the fluid is incompressible and inviscid. The density and kinematic viscosity are denoted by ρ and ν, respectively, and $\mathbf{e}_1$, $\mathbf{e}_2$ and $\mathbf{e}_3$ are the base vectors of Cartesian coordinates in the fluid region V. Here, t is the time. The position vector is $\mathbf{x} = x_i\mathbf{e}_i = x_1\mathbf{e}_1 + x_2\mathbf{e}_2 + x_3\mathbf{e}_3$, and the velocity vector is $\mathbf{u}(\mathbf{x},t) = u_i(\mathbf{x},t)\mathbf{e}_i = u_1\mathbf{e}_1 + u_2\mathbf{e}_2 + u_3\mathbf{e}_3$. The pressure is denoted by $p(\mathbf{x},t)$. The continuity equation and the Navier-Stokes equation in V are, respectively, as

$$\nabla \cdot \mathbf{u} = \sigma, \tag{1}$$

$$\frac{\partial \mathbf{u}}{\partial t} + (\mathbf{u}\cdot\nabla)\mathbf{u} = -\frac{1}{\rho}\nabla p + \nu\nabla^2\mathbf{u}\,, \tag{2}$$

where ∇ is the nabla operator $\mathbf{e}_i\,\partial/\partial x_i$, and σ is the source of fluid per unit volume.

The vorticity $\boldsymbol{\omega}$ is defined as

$$\boldsymbol{\omega} = \nabla\times\mathbf{u}\,. \tag{3}$$

If $(\mathbf{u}\cdot\nabla)\mathbf{u}$ is rewritten according to the vector formula as

$$(\mathbf{u}\cdot\nabla)\mathbf{u} = \frac{1}{2}\nabla(\mathbf{u}\cdot\mathbf{u}) - \mathbf{u}\times\boldsymbol{\omega}\,, \tag{4}$$

then the Navier-Stokes equation, Equation (2), is modified as

$$\frac{\partial \mathbf{u}}{\partial t} + \nabla B - \mathbf{u}\times\boldsymbol{\omega} = -\nu\nabla\times\boldsymbol{\omega} + \nu\nabla\sigma\,, \tag{5}$$

where B is the total pressure and is given as

$$B = \frac{p-p_\infty}{\rho} + \frac{1}{2}(\mathbf{u}\cdot\mathbf{u} - \mathbf{u}_\infty\cdot\mathbf{u}_\infty)\,. \tag{6}$$

If we operate $\nabla\times$ on both sides of Equation (5), we obtain

$$\frac{\partial \boldsymbol{\omega}}{\partial t} - \nabla\times(\mathbf{u}\times\boldsymbol{\omega}) = -\nu\nabla\times(\nabla\times\boldsymbol{\omega})\,. \tag{7}$$

Applying vector formulas, we have

$$\nabla\times(\mathbf{u}\times\boldsymbol{\omega}) = (\boldsymbol{\omega}\cdot\nabla)\mathbf{u} - (\mathbf{u}\cdot\nabla)\boldsymbol{\omega} + \mathbf{u}(\nabla\cdot\boldsymbol{\omega}) - \boldsymbol{\omega}(\nabla\cdot\mathbf{u}) = (\boldsymbol{\omega}\cdot\nabla)\mathbf{u} - (\mathbf{u}\cdot\nabla)\boldsymbol{\omega} - \sigma\boldsymbol{\omega}\,, \tag{8a}$$

$$\nabla\times(\nabla\times\boldsymbol{\omega}) = \nabla(\nabla\cdot\boldsymbol{\omega}) - \nabla^2\boldsymbol{\omega} = -\nabla^2\boldsymbol{\omega}\,, \tag{8b}$$

Equation (7) is then written as

$$\frac{\partial \boldsymbol{\omega}}{\partial t} + (\mathbf{u}\cdot\nabla)\boldsymbol{\omega} = (\boldsymbol{\omega}\cdot\nabla)\mathbf{u} - \sigma\boldsymbol{\omega} + \nu\nabla^2\boldsymbol{\omega}\,. \tag{9}$$

If $\nabla\cdot$ is operated on both sides of Equation (5), we obtain

$$\nabla^2 B - \nabla\cdot(\mathbf{u}\times\boldsymbol{\omega}) = -\frac{\partial\sigma}{\partial t} + \nu\nabla^2\sigma\,. \tag{10}$$

If we assume that the boundary surface S is the body surface and that the fluid velocity on S is $\mathbf{u}_B$, then the boundary condition on S is given by

$$\mathbf{u} = \mathbf{u}_B\,. \tag{11}$$

From Equation (5) , the boundary condition of B becomes

$$\frac{\partial B}{\partial n} \equiv (\nabla B)\cdot\mathbf{n} = \mathbf{n}\cdot\left(-\frac{\partial \mathbf{u}}{\partial t} + \mathbf{u}\times\boldsymbol{\omega} - \nu\nabla\times\boldsymbol{\omega} + \nu\nabla\sigma\right), \tag{12}$$

where $\mathbf{n}$ is the unit outward normal of the boundary surface.

3. IRROTATIONAL FLOWS OR POTENTIAL FLOWS

Let $\mathbf{x} = x_1\mathbf{e}_1 + x_2\mathbf{e}_2 + x_3\mathbf{e}_3 = x_i\mathbf{e}_i$, $\phi(\mathbf{x})$ and $G(\mathbf{x},\boldsymbol{\xi})$ be the coordinates, the velocity potential and the fundamental solution of Laplace operator $\Delta_{\mathbf{x}} = \nabla_{\mathbf{x}}^2 = \partial^2/\partial x_i\partial x_i$ having a singularity at the point $\boldsymbol{\xi} = \xi_i e_i$, respectively. Note that $\phi(\mathbf{x})$ and $G(\mathbf{x},\boldsymbol{\xi})$ satisfy

$$\Delta_{\mathbf{x}}\phi(\mathbf{x}) = \sigma(\mathbf{x})\,, \tag{13}$$

$$\Delta_{\mathbf{x}}G(\mathbf{x},\boldsymbol{\xi}) = \delta(\mathbf{x},\boldsymbol{\xi})\,, \tag{14}$$

where $\delta(\mathbf{x},\boldsymbol{\xi})$ is Dirac's delta function. The fundamental solution $G(\mathbf{x},\boldsymbol{\xi})$ is given by

$$G(\mathbf{x},\boldsymbol{\xi}) = \frac{-1}{4\pi\, r(\mathbf{x},\boldsymbol{\xi})}\,, \tag{15}$$

where $r(\mathbf{x},\boldsymbol{\xi}) = |\,\mathbf{x}-\boldsymbol{\xi}\,|$.

As is well known, the integral representation $G(\mathbf{x},\boldsymbol{\xi})$ of $\phi(\mathbf{x})$ is written as

$$\varepsilon(\mathbf{x})\phi(\mathbf{x}) = -\iint_S\left[G(\mathbf{x},\boldsymbol{\xi})\frac{\partial\phi(\boldsymbol{\xi})}{\partial n_\xi} - \phi(\boldsymbol{\xi})\frac{\partial G(\mathbf{x},\boldsymbol{\xi})}{\partial n_\xi}\right]dS_\xi + \iiint_V G(\mathbf{x},\boldsymbol{\xi})\sigma(\boldsymbol{\xi})\,dV_\xi\,, \tag{16}$$

where

$$\varepsilon(\mathbf{x}) = \begin{cases} 1 & \text{if } \mathbf{x} \text{ in } V \\ 1/2 & \text{if } \mathbf{x} \text{ on } S \\ 0 & \text{otherwise} \end{cases}. \tag{17}$$

For simplicity, we write Equation (16) as

$$\varepsilon\phi = -\iint_S \left[G\frac{\partial \phi}{\partial n} - \phi\frac{\partial G}{\partial n} \right] dS + \iiint_V G\sigma \, dV \,. \tag{18}$$

When $\mathbf{x}$ is in V, from Equation (18), we have

$$\phi = -\iint_S \left[G\frac{\partial \phi}{\partial n} - \phi\frac{\partial G}{\partial n} \right] dS + \iiint_V G\sigma \, dV \,. \tag{19}$$

The velocity vector $\mathbf{u}$ is given by

$$\mathbf{u}(\mathbf{x}) = \nabla_{\mathbf{x}}\phi(\mathbf{x}) = -\iint_S \left[\nabla_{\mathbf{x}} G\frac{\partial \phi}{\partial n} - \phi\frac{\partial \nabla_{\mathbf{x}} G}{\partial n} \right] dS + \iiint_V (\nabla_{\mathbf{x}} G)\sigma \, dV \,, \tag{20}$$

where $\nabla_{\mathbf{x}}$ is $\mathbf{e}_i \partial/\partial x_i$ and

$$\nabla_{\mathbf{x}} G(\mathbf{x},\boldsymbol{\xi}) = \mathbf{G}(\mathbf{x},\boldsymbol{\xi}) = G_i(\mathbf{x},\boldsymbol{\xi})\mathbf{e}_i = \frac{\mathbf{x}-\boldsymbol{\xi}}{4\pi|\,\mathbf{x}-\boldsymbol{\xi}\,|^3} = \frac{\mathbf{r}}{4\pi r^3} \,. \tag{21}$$

And G satisfies

$$\frac{\partial G}{\partial x_i} = -\frac{\partial G}{\partial \xi_i} \quad \text{or} \quad \nabla_{\mathbf{x}} G = -\nabla_{\xi} G \,. \tag{22}$$

Hence, from Equation (20), we have

$$\mathbf{u}(\mathbf{x}) = \nabla_{\mathbf{x}}\phi(\mathbf{x}) = \iint_S \left[\frac{\partial G}{\partial \xi_i}\frac{\partial \phi}{\partial n} - \phi\frac{\partial}{\partial n}\left(\frac{\partial G}{\partial \xi_i}\right) \right] \mathbf{e}_i \, dS + \iiint_V \mathbf{G}\sigma \, dV \,. \tag{23}$$

After lengthy manipulation, we obtain

$$\mathbf{u} = -\iint_S \left[\mathbf{G}(\mathbf{u}\cdot\mathbf{n}) - \mathbf{G}\times(\mathbf{n}\times\mathbf{u}) \right] dS + \iiint_V \mathbf{G}\sigma \, dV \,, \tag{24}$$

where $-\mathbf{u}\cdot\mathbf{n}$ and $\mathbf{n}\times\mathbf{u}$ express the source and vorticity distributions, respectively, on the boundary S. Hence, we know that the velocity vector $\mathbf{u}$ is induced by the source and vorticity distributions on the boundary S and the source distribution σ in V.

4. ROTATIONAL FLOWS OR NON-POTENTIAL FLOWS

In the case of non-potential flows, we consider the velocity vector $\mathbf{u}(\mathbf{x})$ instead of the velocity potential $\phi(\mathbf{x})$. Then, we have the kinematical equations between the velocity vector $\mathbf{u}(\mathbf{x})$ and vorticity $\boldsymbol{\omega}(\mathbf{x})$:

$$\nabla\cdot\mathbf{u}(\mathbf{x}) = \sigma(\mathbf{x}) \,, \tag{25}$$

$$\nabla\times\mathbf{u}(\mathbf{x}) = \boldsymbol{\omega}(\mathbf{x}) \,. \tag{26}$$

If we operate $\nabla\times$ on both sides of Equation (26), we have

$$\nabla^2\mathbf{u}(\mathbf{x}) = \nabla\sigma - \nabla\times\boldsymbol{\omega} \,. \tag{27}$$

We call ∇^2 as the primary space-differential operator. We can apply results similar to Equation (18) to each component of the vector $\mathbf{u}$:

$$\varepsilon\mathbf{u} = -\iint_S \left[G\frac{\partial \mathbf{u}}{\partial n} - \mathbf{u}\frac{\partial G}{\partial n} \right] dS + \iiint_V G(\nabla\sigma - \nabla\times\boldsymbol{\omega}) \, dV \,. \tag{28}$$

In Equation (28), the contributions of the source and vortex are expressed as $\nabla\sigma$ and $\nabla\times\boldsymbol{\omega}$. However, it is favorable if these contributions are given by an expression that does not include the space derivatives of σ and $\boldsymbol{\omega}$. With respect to $G\nabla\sigma$, we use

$$\iiint_V G(\nabla\sigma)\, dV = \iiint_V \left[\nabla(G\sigma) - (\nabla G)\sigma \right] dV = \iint_S G\sigma\mathbf{n}\, dS - \iiint_V (\nabla G)\sigma \, dV \,. \tag{29}$$

With respect to $\nabla\times\boldsymbol{\omega}$, we apply vector formulas:

$$\iiint_V G(\nabla\times\boldsymbol{\omega})\, dV = \iiint_V \left[\nabla\times(G\boldsymbol{\omega}) - (\nabla G)\times\boldsymbol{\omega} \right] dV = \iint_S \mathbf{n}\times(G\boldsymbol{\omega})\, dS - \iiint_V (\nabla G)\times\boldsymbol{\omega} \, dV \,. \tag{30}$$

Substituting Equations (29) and (30) into Equation (28), we obtain

$$\varepsilon\mathbf{u} = -\iint_S \left[G\frac{\partial \mathbf{u}}{\partial n} - \mathbf{u}\frac{\partial G}{\partial n} \right] dS + \iint_S G\sigma\mathbf{n}\, dS - \iint_S \mathbf{n}\times(G\boldsymbol{\omega})\, dS - \iiint_V (\nabla G)\sigma \, dV + \iiint_V (\nabla G)\times\boldsymbol{\omega} \, dV \,. \tag{31}$$

After lengthy manipulation, we obtain from Equation (31)

$$\varepsilon\mathbf{u} = -\iint_S \left[\mathbf{G}(\mathbf{u}\cdot\mathbf{n}) - \mathbf{G}\times(\mathbf{n}\times\mathbf{u})\right]dS + \iiint_V \left[\mathbf{G}\sigma - \mathbf{G}\times\boldsymbol{\omega}\right]dV\,. \tag{32}$$

In the case of flows outside of S, we must take the infinite boundary S_∞ into consideration. We assume that S_∞ is a closed surface and that the flow is uniform at infinity. Since the uniform flow $\mathbf{u}_\infty$ satisfies $\nabla\cdot\mathbf{u}_\infty = 0$ and $\nabla\times\mathbf{u}_\infty = 0$ inside of S_∞, from Equation (24), we have

$$-\iint_{S_\infty} \left[\mathbf{G}(\mathbf{u}_\infty\cdot\mathbf{n}) - \mathbf{G}\times(\mathbf{n}\times\mathbf{u}_\infty)\right]dS = \mathbf{u}_\infty\,. \tag{33}$$

Hence, we obtain

$$\varepsilon\mathbf{u} = -\iint_S \left[\mathbf{G}(\mathbf{u}\cdot\mathbf{n}) - \mathbf{G}\times(\mathbf{n}\times\mathbf{u})\right]dS + \iiint_V \left[\mathbf{G}\sigma - \mathbf{G}\times\boldsymbol{\omega}\right]dV + \mathbf{u}_\infty\,. \tag{34}$$

Equation (34) coincides with the results of Wu and Thompson[1] and Uhlman[5].

We should be cautious in shrinking the calculation region by symmetry, because the infinite boundary becomes open. If we consider the disturbance component, we can neglect the contribution of the infinite boundary and always derive the correct results. When the infinite boundary is not closed, we must modify the integral representation given by Equation (34).

5. INTEGRAL REPRESENTATIONS OF VORTICITY AND TOTAL PRESSURE

Next, we derive the integral representations of the vorticity $\boldsymbol{\omega}$ and the total pressure B. From Equation (9), we have

$$\nabla^2\boldsymbol{\omega} = \frac{1}{\nu}\left[\frac{\partial\boldsymbol{\omega}}{\partial t} + (\mathbf{u}\cdot\nabla)\boldsymbol{\omega} - (\boldsymbol{\omega}\cdot\nabla)\mathbf{u} + \sigma\boldsymbol{\omega}\right]. \tag{35}$$

Using the property of the primary space-differential operator ∇^2, we obtain from Equation (18)

$$\varepsilon\boldsymbol{\omega} = -\iint_S \left[G\frac{\partial\boldsymbol{\omega}}{\partial n} - \boldsymbol{\omega}\frac{\partial G}{\partial n}\right]dS + \frac{1}{\nu}\iiint_V G\left[\frac{\partial\boldsymbol{\omega}}{\partial t} + (\mathbf{u}\cdot\nabla)\boldsymbol{\omega} - (\boldsymbol{\omega}\cdot\nabla)\mathbf{u} + \sigma\boldsymbol{\omega}\right]dV\,. \tag{36}$$

We transform this integral representation into an expression that does not include the space derivatives of $\mathbf{u}$ and $\boldsymbol{\omega}$ as far as possible. Since we have:

$$(\mathbf{u}\cdot\nabla)\boldsymbol{\omega} - (\boldsymbol{\omega}\cdot\nabla)\mathbf{u} = \mathbf{u}(\nabla\cdot\boldsymbol{\omega}) - \boldsymbol{\omega}(\nabla\cdot\mathbf{u}) - \nabla\times(\mathbf{u}\times\boldsymbol{\omega}) = -\sigma\boldsymbol{\omega} - \nabla\times(\mathbf{u}\times\boldsymbol{\omega})\,, \tag{37}$$

$$G\left[\nabla\times(\mathbf{u}\times\boldsymbol{\omega})\right] = \nabla\times\big(G(\mathbf{u}\times\boldsymbol{\omega})\big) - (\nabla G)\times(\mathbf{u}\times\boldsymbol{\omega})\,, \tag{38}$$

from vector formulas, we obtain

$$G\left[(\mathbf{u}\cdot\nabla)\boldsymbol{\omega} - (\boldsymbol{\omega}\cdot\nabla)\mathbf{u}\right] = -G\sigma\boldsymbol{\omega} - \nabla\times\big(G(\mathbf{u}\times\boldsymbol{\omega})\big) + (\nabla G)\times(\mathbf{u}\times\boldsymbol{\omega})\,. \tag{39}$$

Substituting Equation (39) into Equation (36), we have

$$\varepsilon\boldsymbol{\omega} = -\iint_S \left[G\frac{\partial\boldsymbol{\omega}}{\partial n} - \boldsymbol{\omega}\frac{\partial G}{\partial n}\right]dS + \frac{1}{\nu}\iiint_V G\frac{\partial\boldsymbol{\omega}}{\partial t}dV + \frac{1}{\nu}\iiint_V \left[-\nabla\times\big(G(\mathbf{u}\times\boldsymbol{\omega})\big) + (\nabla G)\times(\mathbf{u}\times\boldsymbol{\omega})\right]dV\,. \tag{40}$$

Applying a vector integral formula, we obtain

$$\varepsilon\boldsymbol{\omega} = -\iint_S \left[G\frac{\partial\boldsymbol{\omega}}{\partial n} - \boldsymbol{\omega}\frac{\partial G}{\partial n}\right]dS - \frac{1}{\nu}\iint_S G\left[\mathbf{n}\times(\mathbf{u}\times\boldsymbol{\omega})\right]dS + \frac{1}{\nu}\iiint_V \left[G\frac{\partial\boldsymbol{\omega}}{\partial t} + (\nabla G)\times(\mathbf{u}\times\boldsymbol{\omega})\right]dV\,. \tag{41}$$

Furthermore, since $\mathbf{G} = \nabla_{\mathbf{x}}G = -\nabla_{\boldsymbol{\xi}}G$, the integral representation of $\boldsymbol{\omega}$ can be written as

$$\varepsilon\boldsymbol{\omega} = -\iint_S \left[G\frac{\partial\boldsymbol{\omega}}{\partial n} + \boldsymbol{\omega}(\mathbf{G}\cdot\mathbf{n})\right]dS - \frac{1}{\nu}\iint_S G\left[\mathbf{n}\times(\mathbf{u}\times\boldsymbol{\omega})\right]dS + \frac{1}{\nu}\iiint_V \left[G\frac{\partial\boldsymbol{\omega}}{\partial t} - \mathbf{G}\times(\mathbf{u}\times\boldsymbol{\omega})\right]dV\,. \tag{42}$$

This integral representation includes a space derivative $\partial\boldsymbol{\omega}/\partial n$ in a boundary integral.

The integral representation given by Equation (42) is shown to be equal to the following representation by Uhlman [5].

$$\begin{aligned}\varepsilon\boldsymbol{\omega} &= -\iint_S \left[\mathbf{G}(\boldsymbol{\omega}\cdot\mathbf{n}) - \mathbf{G}\times(\mathbf{n}\times\boldsymbol{\omega})\right]dS + \frac{1}{\nu}\iint_S B(\mathbf{G}\times\mathbf{n})\,dS - \iint_S \sigma(\mathbf{G}\times\mathbf{n})\,dS \\ &\quad + \frac{1}{\nu}\iiint_{\cdots V}\left[-\nabla\times\left(G\frac{\partial\mathbf{u}}{\partial t}\right) + G\frac{\partial\boldsymbol{\omega}}{\partial t} - \mathbf{G}\times(\mathbf{u}\times\boldsymbol{\omega})\right]dV \\ &= -\iint_S \left[\mathbf{G}(\boldsymbol{\omega}\cdot\mathbf{n}) - \mathbf{G}\times(\mathbf{n}\times\boldsymbol{\omega})\right]dS + \frac{1}{\nu}\iint_S B(\mathbf{G}\times\mathbf{n})\,dS - \iint_S \sigma(\mathbf{G}\times\mathbf{n})\,dS \\ &\quad - \frac{1}{\nu}\iint_S G\left(\mathbf{n}\times\frac{\partial\mathbf{u}}{\partial t}\right)dS + \frac{1}{\nu}\iiint_V \left[G\frac{\partial\boldsymbol{\omega}}{\partial t} - \mathbf{G}\times(\mathbf{u}\times\boldsymbol{\omega})\right]dV\,.\end{aligned} \tag{43}$$

Uhlman's expression does not include any space derivatives of variables $\mathbf{u}$, $\boldsymbol{\omega}$ and B.

We now obtain the integral representation of B below. Again, We write the differential equation given by Equation (10) and the boundary condition given by Equation (12):

$$\nabla^2(B-\nu\sigma)=\nabla\cdot(\mathbf{u}\times\boldsymbol{\omega})-\frac{\partial\sigma}{\partial t}\ \text{in}\ V\ , \tag{44}$$

$$\frac{\partial(B-\nu\sigma)}{\partial n}=\mathbf{n}\cdot\left(-\frac{\partial\mathbf{u}}{\partial t}+\mathbf{u}\times\boldsymbol{\omega}-\nu\nabla\times\boldsymbol{\omega}\right)\ \text{on}\ S\ . \tag{45}$$

Hence, using the property of the primary space-differential operator ∇^2, we obtain from Equation (18)

$$\varepsilon(B-\nu\sigma)=-\iint_S\left[G\mathbf{n}\cdot\left(-\frac{\partial\mathbf{u}}{\partial t}+\mathbf{u}\times\boldsymbol{\omega}-\nu\nabla\times\boldsymbol{\omega}\right)\right]dS+\iint_S(B-\nu\sigma)\frac{\partial G}{\partial n}dS+\iiint_V G\left[\nabla\cdot(\mathbf{u}\times\boldsymbol{\omega})-\frac{\partial\sigma}{\partial t}\right]dV\ . \tag{46}$$

Equation (46) is shown to be equal to the integral representation of B obtained by Uhlman [5]:

$$\varepsilon(B-\nu\sigma)-\iint_S(B-\nu\sigma)\frac{\partial G}{\partial n}dS=\iint_S\left[\mathbf{n}\cdot\frac{\partial\mathbf{u}}{\partial t}G+\nu\nabla G\cdot(\mathbf{n}\times\boldsymbol{\omega})\right]dS-\iiint_V\left[\left[\nabla G\cdot(\mathbf{u}\times\boldsymbol{\omega})\right]+G\frac{\partial\sigma}{\partial t}\right]dV\ . \tag{47}$$

6. GENERAL RESULTS INCLUDING RESULTS OTHER THAN 3D RESULTS

We generalize the integral representations in 3D obtained above to other dimensions following Wu and Thompson [1]. With respect to velocity $\mathbf{u}$, Equation (32) is generalized as

$$\begin{aligned}\varepsilon\mathbf{u}(\mathbf{x},t)=-A\Bigg[&\int_S\frac{(\mathbf{x}-\boldsymbol{\xi})(\mathbf{u}(\boldsymbol{\xi},t)\cdot\mathbf{n}_\xi)}{|\mathbf{x}-\boldsymbol{\xi}|^d}dS_\xi-\int_S\frac{(\mathbf{x}-\boldsymbol{\xi})\times(\mathbf{n}_\xi\times\mathbf{u}(\boldsymbol{\xi},t))}{|\mathbf{x}-\boldsymbol{\xi}|^d}dS_\xi\\&-\int_V\frac{(\mathbf{x}-\boldsymbol{\xi})\sigma(\boldsymbol{\xi},t)}{|\mathbf{x}-\boldsymbol{\xi}|^d}dV_\xi+\int_V\frac{(\mathbf{x}-\boldsymbol{\xi})\times\boldsymbol{\omega}(\boldsymbol{\xi},t)}{|\mathbf{x}-\boldsymbol{\xi}|^d}dV_\xi\Bigg]+C\ ,\end{aligned} \tag{48}$$

where V refers to the volume area in 3D, the surface area in 2D and the line area in 1D, respectively, and S refers to the boundary surface in 3D, the boundary line in 2D and the boundary point in 1D. Moreover, A and C are defined as follows

$$A=\begin{cases}1/4\pi\ \text{ and }\ d=3\ \textbf{in}\ 3D\\1/2\pi\ \text{ and }\ d=2\ \textbf{in}\ 2D\\1/2\ \text{ and }\ d=1\ \textbf{in}\ 1D\end{cases},\quad C=\begin{cases}0\ \text{for flows interior of}\ S\\\mathbf{u}_\infty\ \text{for flows exterior of}\ S\end{cases}. \tag{49}$$

With respect to the vorticity $\boldsymbol{\omega}$, we generalize Equation (42) as

$$\begin{aligned}\varepsilon(\mathbf{x})\boldsymbol{\omega}(\mathbf{x},t)=&-\int_S G(\mathbf{x},\boldsymbol{\xi})\frac{\partial\boldsymbol{\omega}(\boldsymbol{\xi},t)}{\partial n_\xi}dS_\xi-A\int_S\frac{\boldsymbol{\omega}(\boldsymbol{\xi},t)\big((\mathbf{x}-\boldsymbol{\xi})\cdot\mathbf{n}_\xi\big)}{|\mathbf{x}-\boldsymbol{\xi}|^d}dS_\xi\\&-\frac{1}{\nu}\int_S G(\mathbf{x},\boldsymbol{\xi})\big[\mathbf{n}_\xi\times(\mathbf{u}(\boldsymbol{\xi},t)\times\boldsymbol{\omega}(\boldsymbol{\xi},t))\big]dS_\xi\\&+\frac{1}{\nu}\int_V G(\mathbf{x},\boldsymbol{\xi})\frac{\partial\boldsymbol{\omega}(\boldsymbol{\xi},t)}{\partial t}dV_\xi-A\frac{1}{\nu}\int_V\frac{(\mathbf{x}-\boldsymbol{\xi})\times(\mathbf{u}(\boldsymbol{\xi},t)\times\boldsymbol{\omega}(\boldsymbol{\xi},t))}{|\mathbf{x}-\boldsymbol{\xi}|^d}dV_\xi\ ,\end{aligned} \tag{50}$$

where

$$G(\mathbf{x},\boldsymbol{\xi})=\begin{cases}-(1/4\pi)\,|\mathbf{x}-\boldsymbol{\xi}|^{-1}\ \text{ and }\ d=3\ \textbf{in}\ 3D\\(1/2\pi)\ln(|\mathbf{x}-\boldsymbol{\xi}|)\ \text{ and }\ d=2\ \textbf{in}\ 2D\\(1/2)\,|\mathbf{x}-\boldsymbol{\xi}|\ \text{ and }\ d=1\ \textbf{in}\ 1D\end{cases}. \tag{51}$$

If we generalize Equation (43) obtained originally by Uhlman [5], we obtain

$$\begin{aligned}\varepsilon(\mathbf{x})\boldsymbol{\omega}(\mathbf{x},t)=-A\Bigg\{&\int_S\left[\frac{(\mathbf{n}_\xi\cdot\boldsymbol{\omega}(\boldsymbol{\xi},t))(\mathbf{x}-\boldsymbol{\xi})}{|\mathbf{x}-\boldsymbol{\xi}|^d}-\frac{(\mathbf{x}-\boldsymbol{\xi})\times(\mathbf{n}_\xi\times\boldsymbol{\omega}(\boldsymbol{\xi},t))}{|\mathbf{x}-\boldsymbol{\xi}|^d}\right]dS_\xi\\&-\frac{1}{\nu}\int_S B(\boldsymbol{\xi},t)\frac{(\mathbf{x}-\boldsymbol{\xi})\times\mathbf{n}_\xi}{|\mathbf{x}-\boldsymbol{\xi}|^d}dS_\xi+\int_S\sigma(\boldsymbol{\xi},t)\frac{(\mathbf{x}-\boldsymbol{\xi})\times\mathbf{n}_\xi}{|\mathbf{x}-\boldsymbol{\xi}|^d}dS_\xi\Bigg\}\\&-\frac{1}{\nu}\int_S\left(\mathbf{n}_\xi\times\frac{\partial\mathbf{u}(\boldsymbol{\xi},t)}{\partial t}\right)G(\mathbf{x},\boldsymbol{\xi})\,dS_\xi\\&+\frac{1}{\nu}\int_V\frac{\partial\boldsymbol{\omega}(\boldsymbol{\xi},t)}{\partial t}G(\mathbf{x},\boldsymbol{\xi})\,dV_\xi-A\frac{1}{\nu}\int_V\frac{(\mathbf{x}-\boldsymbol{\xi})\times(\mathbf{u}(\boldsymbol{\xi},t)\times\boldsymbol{\omega}(\boldsymbol{\xi},t))}{|\mathbf{x}-\boldsymbol{\xi}|^d}dV_\xi\ .\end{aligned} \tag{52}$$

In 1D flow, the second surface integral including B on the right-hand side should be replaced by $\frac{1}{\rho}\frac{dp}{dx}(L-2y)\mathbf{e}_3$ considering the contribution from the infinite boundary.

With respect to the total pressure B, Equation (47) obtained originally by Uhlman [5] is generalized as

$$\begin{aligned}\varepsilon(\mathbf{x})[B(\mathbf{x},t)-\nu\sigma(\mathbf{x},t)]-\int_S[B(\xi,t)-\nu\sigma(\xi,t)]\frac{\partial G(\mathbf{x},\xi)}{\partial n_\xi}dS_\xi \\ =\int_S\left(\mathbf{n}_\xi\cdot\frac{\partial\mathbf{u}(\xi,t)}{\partial t}\right)G(\mathbf{x},\xi)dS_\xi-A\int_S\nu\frac{(\mathbf{x}-\xi)\cdot(\mathbf{n}_\xi\times\boldsymbol{\omega}(\xi,t))}{|\mathbf{x}-\xi|^d}dS_\xi \\ +A\int_V\frac{(\mathbf{x}-\xi)\cdot(\mathbf{u}(\xi,t)\times\boldsymbol{\omega}(\xi,t))}{|\mathbf{x}-\xi|^d}dV_\xi-\int_V\frac{\partial\sigma(\xi,t)}{\partial t}G(\mathbf{x},\xi)\,dV_\xi\,. \end{aligned} \quad (53)$$

7. SOLUTIONS USING INTEGRAL REPRESENTATIONS

The integral representations given by Equations (48), (52) and (53) do not include the space derivatives of $\mathbf{u}$, $\boldsymbol{\omega}$ and B in any of the regional and boundary integrals. Hence, if we use the integral representations, we can derive a numerical solution of flow that does not require the space derivatives. The integral representation given by Equation (50) does not include the space derivatives in the region but does include the normal derivative of $\boldsymbol{\omega}$ on the boundary.

The solutions of flow using the integral representations are summarized below.

Solution A1. Explicit solution

A1.1. Solution using the integral representations given by Equations (48), (50) and (53):

(1) Assume $\boldsymbol{\omega}(\mathbf{x},t)$ at time t.

(2) Obtain $\mathbf{u}(\mathbf{x},t)$ using Equation (48).

(3) Solve the integral equation given in Equation (50) for $\partial\boldsymbol{\omega}(\mathbf{x},t)/\partial t$.

(4) Obtain $\boldsymbol{\omega}(\mathbf{x},t+dt)$ from $\boldsymbol{\omega}(\mathbf{x},t+dt)=\boldsymbol{\omega}(\mathbf{x},t)+(\partial\boldsymbol{\omega}(\mathbf{x},t)/\partial t)dt$.

(5) Make the time $t+dt$ and repeat the process.

Solve $B(\mathbf{x},t)$ from the boundary integral equation given in Equation (53) in parallel.

A1.2. Solution using the integral representations given by Equations (48), (52) and (53):

(1) Assume $\boldsymbol{\omega}(\mathbf{x},t)$ at time t.

(2) Obtain $\mathbf{u}(\mathbf{x},t)$ using Equation (48).

(3) Solve the boundary integral equation given in Equation (53) for $B(\mathbf{x},t)$.

(4) Solve the integral equation given in Equation (52) for $\partial\boldsymbol{\omega}(\mathbf{x},t)/\partial t$.

(5) Obtain $\boldsymbol{\omega}(\mathbf{x},t+dt)$ from $\boldsymbol{\omega}(\mathbf{x},t+dt)=\boldsymbol{\omega}(\mathbf{x},t)+(\partial\boldsymbol{\omega}(\mathbf{x},t)/\partial t)dt$.

(6) Make the time $t+dt$ and repeat the process.

Solution A2. Implicit solution

A2.1. Solution using the integral representations given by Equations (48), (50) and (53):

(1) Assume $\boldsymbol{\omega}(\mathbf{x},t)$ and $\mathbf{u}(\mathbf{x},t)$ at time t.

(2) At $t+dt$, approximate $\partial\boldsymbol{\omega}(\mathbf{x},t+dt)/\partial t$ by $\partial\boldsymbol{\omega}(\mathbf{x},t+dt)/\partial t=[\boldsymbol{\omega}(\mathbf{x},t+dt)-\boldsymbol{\omega}(\mathbf{x},t)]/dt$ in Equation (50) and solve the simultaneous integral equations given in (48) and (50) for $\mathbf{u}(\mathbf{x},t+dt)$ and $\boldsymbol{\omega}(\mathbf{x},t+dt)$.

(3) Make the time $t+2dt$. Then, return to Step (2) and repeat the process.

Solve $B(\mathbf{x},t)$ from the boundary integral equation given in Equation (53) in parallel.

As an alternative to solving the integral equations simultaneously, an iteration may be applied. Namely, we approximate $\mathbf{u}(\mathbf{x},t+dt)$ by $\mathbf{u}(\mathbf{x},t)$ and solve the integral equation given in Equation (50) for $\boldsymbol{\omega}(\mathbf{x},t+dt)$. Using $\boldsymbol{\omega}(\mathbf{x},t+dt)$, we renew $\mathbf{u}(\mathbf{x},t+dt)$ by Equation (48). Then, using $\mathbf{u}(\mathbf{x},t+dt)$, we again solve the integral equation given in Equation (50) for $\boldsymbol{\omega}(\mathbf{x},t+dt)$. We repeat this process until convergence.

A2.2. Solution using the integral representations given by Equations (48), (52) and (53):

(1) Assume $\boldsymbol{\omega}(\mathbf{x},t)$ and $\mathbf{u}(\mathbf{x},t)$ at time t.

(2) At $t+dt$, approximate $\partial\boldsymbol{\omega}(\mathbf{x},t+dt)/\partial t$ by $\partial\boldsymbol{\omega}(\mathbf{x},t+dt)/\partial t=[\boldsymbol{\omega}(\mathbf{x},t+dt)-\boldsymbol{\omega}(\mathbf{x},t)]/dt$ in Equation (52) and

solve the simultaneous integral equations given in Equations (48), (52) and (53) for $\mathbf{u}(\mathbf{x},t+dt)$, $\boldsymbol{\omega}(\mathbf{x},t+dt)$ and $B(\mathbf{x},t+dt)$.

(3) Make the time $t+2dt$. Then, return to Step (2) and repeat the process.

As an alternative to solving integral equations simultaneously, an iteration may be applied. Namely, we approximate $\mathbf{u}(\mathbf{x},t+dt)$ and $B(\mathbf{x},t+dt)$ by $\mathbf{u}(\mathbf{x},t)$ and $B(\mathbf{x},t)$, respectively, and solve the integral equation given in Equation (52) for $\boldsymbol{\omega}(\mathbf{x},t+dt)$. By using $\boldsymbol{\omega}(\mathbf{x},t+dt)$, we renew $\mathbf{u}(\mathbf{x},t+dt)$ and $B(\mathbf{x},t+dt)$ by Equation (48) and the boundary integral equation given in Equation (53), respectively. Then, using $\mathbf{u}(\mathbf{x},t+dt)$ and $B(\mathbf{x},t+dt)$, we again solve the integral equation given in Equation (52) for $\boldsymbol{\omega}(\mathbf{x},t+dt)$. We repeat this process until convergence.

7.1. Applications to 1D flows

As special cases of 2D flows, there are flows with $\mathbf{u}=u(y,t)\mathbf{e}_1$ and $\nabla p = dp/dx\mathbf{e}_1 = \text{const}$. In other word, these flows are 1D flows such as the Rayleigh flow, the Couette flow and the Hagen-Poiseuille flow. In these cases, the vorticity $\boldsymbol{\omega}$ is directed toward $z-$axis or $\boldsymbol{\omega}=\omega(y,t)\mathbf{e}_3$. In the following discussions, we assume $\sigma=0$.

The flow region is $0<y<L$. The equation of continuity is satisfied automatically, and Equations (3) and (5) become

$$\omega\mathbf{e}_3 = -\frac{\partial u}{\partial y}\mathbf{e}_3 \text{ or } \frac{\partial u}{\partial y} = -\omega \text{ in } 0<y<L, \tag{54}$$

$$\frac{\partial u}{\partial t}\mathbf{e}_1 = -\left(\nu\frac{\partial \omega}{\partial y}+\frac{1}{\rho}\frac{dp}{dx}\right)\mathbf{e}_1 \text{ or } \frac{\partial \omega}{\partial y} = -\frac{1}{\nu}\left(\frac{\partial u}{\partial t}+\frac{1}{\rho}\frac{dp}{dx}\right) \text{ in } 0<y<L. \tag{55}$$

If we apply the integral representation given by Equation (48) for velocity $\mathbf{u}$, we have

$$\mathbf{x}-\boldsymbol{\xi}=(y-\eta)\mathbf{e}_2,\ \mathbf{n}(\boldsymbol{\xi})=\begin{cases}\mathbf{e}_2 & \text{on } y=L\\ -\mathbf{e}_2 & \text{on } y=0\end{cases}, \tag{56}$$

$$\begin{aligned}\varepsilon(\mathbf{x})\mathbf{u}(\mathbf{x},t) &= -\frac{1}{2}\int_V \frac{(\mathbf{x}-\boldsymbol{\xi})\times\boldsymbol{\omega}(\boldsymbol{\xi},t)}{|\mathbf{x}-\boldsymbol{\xi}|}dV_\xi + \frac{1}{2}\left[\frac{(\mathbf{x}-\boldsymbol{\xi})\times(\mathbf{n}(\boldsymbol{\xi})\times\mathbf{u}(\boldsymbol{\xi},t))}{|\mathbf{x}-\boldsymbol{\xi}|}\right]_{\xi=L\mathbf{e}_2} + \frac{1}{2}\left[\frac{(\mathbf{x}-\boldsymbol{\xi})\times(\mathbf{n}(\boldsymbol{\xi})\times\mathbf{u}(\boldsymbol{\xi},t))}{|\mathbf{x}-\boldsymbol{\xi}|}\right]_{\xi=0}\\ &= -\frac{1}{2}\int_0^L \text{sgn}(y-\eta)\mathbf{e}_2\times\omega(\eta,t)\mathbf{e}_3 d\eta + \frac{1}{2}\left[\text{sgn}(y-L)\mathbf{e}_2\times(\mathbf{e}_2\times u(L,t)\mathbf{e}_1)\right] + \frac{1}{2}\left[\text{sgn}(y)\mathbf{e}_2\times(-\mathbf{e}_2\times u(0,t)\mathbf{e}_1)\right]\\ &= -\frac{1}{2}\int_0^L \text{sgn}(y-\eta)\omega(\eta,t)d\eta\,\mathbf{e}_1 - \frac{1}{2}\text{sgn}(y-L)u(L,t)\mathbf{e}_1 + \frac{1}{2}\text{sgn}(y)u(0,t)\mathbf{e}_1.\end{aligned} \tag{57}$$

Hence, we obtain

$$\varepsilon u(y,t) = -\frac{1}{2}\int_0^L \text{sgn}(y-\eta)\omega(\eta,t)d\eta + \frac{1}{2}\text{sgn}(L-y)u(L,t) + \frac{1}{2}\text{sgn}(y)u(0,t). \tag{58}$$

If we apply the integral representation given by Equation (52) for vorticity $\boldsymbol{\omega}$, we have

$$\begin{aligned}\varepsilon(y)\omega(y,t) &= \frac{1}{2\nu}\int_0^L \frac{\partial\omega(\eta,t)}{\partial t}|y-\eta|d\eta + \frac{1}{2\rho\nu}\frac{dp}{dx}(L-2y)\\ &\quad + \frac{1}{2}\text{sgn}(L-y)\omega(L,t) + \frac{1}{2}\text{sgn}(y)\omega(0,t) + \frac{1}{2\nu}\frac{\partial u(L,t)}{\partial t}|L-y| - \frac{1}{2\nu}\frac{\partial u(0,t)}{\partial t}|y|.\end{aligned} \tag{59}$$

If we apply Equation (55), Equation (59) can be rewritten as

$$\begin{aligned}\varepsilon(y)\omega(y,t) &= \frac{1}{2\nu}\int_0^L \frac{\partial\omega(\eta,t)}{\partial t}|y-\eta|d\eta + \frac{1}{2}\text{sgn}(L-y)\omega(L,t) + \frac{1}{2}\text{sgn}(y)\omega(0,t)\\ &\quad - \frac{1}{2}\frac{\partial\omega(L,t)}{\partial y}|L-y| + \frac{1}{2}\frac{\partial\omega(0,t)}{\partial y}|y|.\end{aligned} \tag{60}$$

The integral representation given by Equation (60) is simply the 1D integral representation obtained by Equation (50)

If we apply the integral representation given by Equation (53) for B, we have

$$\varepsilon(y)B(y,t) - \frac{1}{2}\text{sgn}(L-y)B(L,t) - \frac{1}{2}\text{sgn}(y)B(0,t) = -\frac{1}{2}\int_0^L \text{sgn}(y-\eta)u(\eta,t)\omega(\eta,t)d\eta. \tag{61}$$

We transform the 1D integral representations into algebraic equations. For simplicity, we divide the region $0\le y\le L$ into N equal elements of length dy and denote the midpoint of each element as y_i, $i=0,1,\cdots,N-1$. Thus, we have

$$dy = \frac{L}{N} \tag{62}$$

and

$$y_i = (0.5+i)dy. \tag{63}$$

We approximate Equation (60) as

$$\varepsilon(y)\omega(y,t)=\frac{1}{2\nu}\sum_{j=0}^{j=N-1}\frac{\partial\omega(y_j,t)}{\partial t}\int_{y_j-dy/2}^{y_j-dy/2}|y-\eta|d\eta$$
$$+\frac{1}{2}\mathrm{sgn}(L-y)\omega(L,t)+\frac{1}{2}\mathrm{sgn}(y)\omega(0,t)-\frac{1}{2}\frac{\partial\omega(L,t)}{\partial y}|L-y|+\frac{1}{2}\frac{\partial\omega(0,t)}{\partial y}|y|. \quad (64)$$

We define α_{ij} for IP $y=y_i$ and α_{BPj} for BP $y=0$ or $y=L$ as

$$\alpha_{ij}=\int_{y_j-dy/2}^{y_j-dy/2}|y_i-\eta|d\eta=\begin{cases}dy^2/4 & \text{when } i=j\\ |y_i-y_j|dy & \text{when } i\neq j\end{cases}, \quad (65a)$$

$$\alpha_{BPj}=\int_{y_j-dy/2}^{y_j+dy/2}|y_{BP}-\eta|d\xi=|y_{BP}-y_j|dy. \quad (65b)$$

Then, we obtain then the algebraic equations for IP (y_i, $i=0,1,\cdots,N-1$) and BP ($y_{BP}=0, L$), respectively, as

$$\omega(y_i,t)=\frac{1}{2\nu}\sum_{j=0}^{j=N-1}\alpha_{ij}\frac{\partial\omega(y_j,t)}{\partial t}+\frac{1}{2}\mathrm{sgn}(L-y_i)\omega(L,t)+\frac{1}{2}\mathrm{sgn}(y_i)\omega(0,t)$$
$$-\frac{1}{2}|L-y_i|\frac{\partial\omega(L,t)}{\partial y}+\frac{1}{2}|y_i|\frac{\partial\omega(0,t)}{\partial y}, \quad (66a)$$

$$\frac{1}{2}\omega(y_{BP},t)=\frac{1}{2\nu}\sum_{j=0}^{j=N-1}\alpha_{BPj}\frac{\partial\omega(y_j,t)}{\partial t}+\frac{1}{2}\mathrm{sgn}(L-y_{BP})\omega(L,t)+\frac{1}{2}\mathrm{sgn}(y_{BP})\omega(0,t)$$
$$-\frac{1}{2}|L-y_{BP}|\frac{\partial\omega(L,t)}{\partial y}+\frac{1}{2}|y_{BP}|\frac{\partial\omega(0,t)}{\partial y}. \quad (66b)$$

In the case of Solution A1.1, the algebraic equations and the time progression equation are given by

$$2\nu\left[\omega(y_i,t)-\frac{1}{2}\mathrm{sgn}(L-y_i)\omega(L,t)-\frac{1}{2}\mathrm{sgn}(y_i)\omega(0,t)\right.$$
$$\left.+\frac{1}{2}\frac{\partial\omega(L,t)}{\partial y}|L-y_i|-\frac{1}{2}\frac{\partial\omega(0,t)}{\partial y}|y_i|\right]=\sum_{j=0}^{N-1}\alpha_{ij}\frac{\partial\omega(y_j,t)}{\partial t}, \quad (67a)$$

$$2\nu\left[\frac{1}{2}\omega(y_{BP},t)-\frac{1}{2}\mathrm{sgn}(L-y_{BP})\omega(L,t)-\frac{1}{2}\mathrm{sgn}(y_{BP})\omega(0,t)\right.$$
$$\left.+\frac{1}{2}\frac{\partial\omega(L,t)}{\partial y}|L-y_{BP}|-\frac{1}{2}\frac{\partial\omega(0,t)}{\partial y}|y_{BP}|\right]=\sum_{j=0}^{N-1}\alpha_{BPj}\frac{\partial\omega(y_j,t)}{\partial t}, \quad (67b)$$

$$\omega(y_i,t+dt)=\omega(y_i,t)+\frac{\partial\omega(y_i,t)}{\partial t}dt. \quad (67c)$$

The total number of the unknowns of the algebraic equations is $N+2$: $\partial\omega(y_j,t)/\partial t$ for $j=0,1,\cdots,N-1$, and $\omega(0,t)$ or $\partial\omega(0,t)/\partial y$ and $\omega(L,t)$ or $\partial\omega(L,t)/\partial y$. The total number of equations is also $N+2$: N for IP and 2 for BP.

In this case, all of the unknown variables on IP and BP become unknowns. In other words, the method is a region+boundary element method.

As an approximation, we use $\partial\omega(0,t)/\partial y\approx 2[\omega(y_0,t)-\omega(0,t)]/dy$, if $\omega(0,t)$ is known. Otherwise, we use $\omega(0,t)\approx\omega(y_0,t)-\partial\omega(0,t)/\partial y\cdot dy/2$, if $\partial\omega(0,t)/\partial y$ is known. We use similar approximations for $x=L$. In this case, the number of unknowns and the number of equation are both N.

In the case of Solution A2.1, the algebraic equations are given by

$$2\nu dt\left[\omega(y_i,t+dt)-\frac{1}{2}\mathrm{sgn}(L-y_i)\omega(L,t+dt)-\frac{1}{2}\mathrm{sgn}(y_i)\omega(0,t+dt)\right.$$
$$\left.+\frac{1}{2}\frac{\partial\omega(L,t+dt)}{\partial y}|L-y_i|-\frac{1}{2}\frac{\partial\omega(0,t+dt)}{\partial y}|y_i|\right]=\sum_{j=0}^{N-1}\alpha_{ij}\omega(y_j,t+dt)-\sum_{j=0}^{N-1}\alpha_{ij}\omega(y_j,t), \quad (68a)$$

$$2\nu dt\left[\frac{1}{2}\omega(y_{BP},t+dt)-\frac{1}{2}\mathrm{sgn}(L-y_{BP})\omega(L,t+dt)-\frac{1}{2}\mathrm{sgn}(y_{BP})\omega(0,t+dt)\right.$$
$$\left.+\frac{1}{2}\frac{\partial\omega(L,t+dt)}{\partial y}|L-y_{BP}|-\frac{1}{2}\frac{\partial\omega(0,t+dt)}{\partial y}|y_{BP}|\right]=\sum_{j=0}^{N-1}\alpha_{BPj}\omega(y_j,t+dt)-\sum_{j=0}^{N-1}\alpha_{BPj}\omega(y_j,t). \quad (68b)$$

The total number of unknowns of the algebraic equations is $N+2$: $\omega(y_j,t+dt)$ for $j=0,1,\cdots,N-1$, and $\omega(0,t+dt)$ or $\partial\omega(0,t+dt)/\partial y$ and $\omega(L,t+dt)$ or $\partial\omega(L,t+dt)/\partial y$. The total number of equations is also $N+2$: N for IP and 2 for BP.

In this case, we can also obtain the values of the unknown variables on BP from Equation (68b) assuming that the values of the unknown variables on IP are known. Substituting the values of the unknown variables on BP into Equation (68a), we again update the values of the unknown variables on IP. Then, we again substitute the new values of the unknown variables on IP into Equation (68b) for the new values of the unknown variables on BP. We can consider this type of iterative scheme, which corresponds to Boundary Element Method + Iteration (BEMI).

As an approximation, we use $\partial\omega(0,t+dt)/\partial y \approx 2[\omega(y_0,t+dt)-\omega(0,t+dt)]/dy$, if $\omega(0,t+dt)$ is known. Otherwise, we use $\omega(0,t+dt)\approx\omega(y_0,t+dt)-\partial\omega(0,t+dt)/\partial y\cdot dy/2$, if $\partial\omega(0,t+dt)/\partial y$ is known. We use similar approximations for $x=L$. In this case, the number of unknowns and the number of equations are both N .

7.1.1. Hagen-Poiseuille flow

We take the $x-$axis to be in the horizontal direction and the $y-$axis to be perpendicular to the $x-$axis. There are two plates placed on the $y=0$ and $y=L$ planes. Both the lower plate on $y=0$ and the upper plate on $y=L$ are fixed. Instantly, we apply the constant pressure gradient dp/dx to the fluid in $0<y<L$. We observe the fluid motion in $0<y<L$ relative to coordinates fixed to the plates. The flow is one-dimensional and satisfies $u=u(y,t)$, $v=0$, and, $\partial p/\partial x=\text{const}$. The conditions are summarized below.

Pressure gradient: 0 .

$$\text{Initial value: From } u(y_i,0)=0,\ \omega(y_i,0)=0, \tag{69}$$

$$\text{Boundary value: From } u(0,t)=u(L,t)=0,\ \frac{\partial\omega(0,t)}{\partial y}=\frac{\partial\omega(L,t)}{\partial y}=-\frac{1}{\rho\nu}\frac{dp}{dx}, \tag{70}$$

$$\text{Approximation: } \omega(0,t)\approx\omega(y_0,t),\ \omega(L,t)\approx\omega(y_{N-1},t), \tag{71}$$

where Equation (55) yields the second equation in Equation (70). In case of Solution A1.1, Equations (67a) and (67c) yield

$$2\nu\left[\omega(y_i,t)+\frac{1}{2\rho\nu}\frac{dp}{dx}(2y_i-L)-\frac{1}{2}\omega(y_0,t)-\frac{1}{2}\omega(y_{N-1},t)\right]=\sum_{j=0}^{N-1}\alpha_{ij}\frac{\partial\omega(y_j,t)}{\partial t},\ i=0,1,\cdots,N-1, \tag{72a}$$

$$\omega(y_i,t+dt)=\omega(y_i,t)+\frac{\partial\omega(y_i,t)}{\partial t}dt,\ i=0,1,\cdots,N-1. \tag{72b}$$

In case of Solution A2.1, Equation (68a) yields

$$\begin{aligned}&2\nu dt\left[\omega(y_i,t+dt)+\frac{1}{2\rho\nu}\frac{dp}{dx}(2y_i-L)-\frac{1}{2}\omega(y_0,t+dt)-\frac{1}{2}\omega(y_{N-1},t+dt)\right]\\&=\sum_{j=0}^{N-1}\alpha_{ij}\omega(y_j,t+dt)-\sum_{j=0}^{N-1}\alpha_{ij}\omega(y_j,t),\ i=0,1,\cdots,N-1.\end{aligned} \tag{73}$$

The steady state solution of the problem is given by

$$\omega=-\frac{1}{2\rho\nu}\frac{dp}{dx}(2y-L) \tag{74a}$$

$$u=\frac{1}{2\rho\nu}\frac{dp}{dx}y(y-L) \tag{74b}$$

We used Solution A1.1 for the numerical calculation. Numerical results are shown in Figure 1. The calculation conditions are $dp/dx=-1000$, $L=1$, $N=20$, $dt=0.0005$, and $\nu=0.089$. The broken lines indicate the results for the steady state given by Equation (74). Figure 1(d) shows that the correct steady state is obtained when t is large.

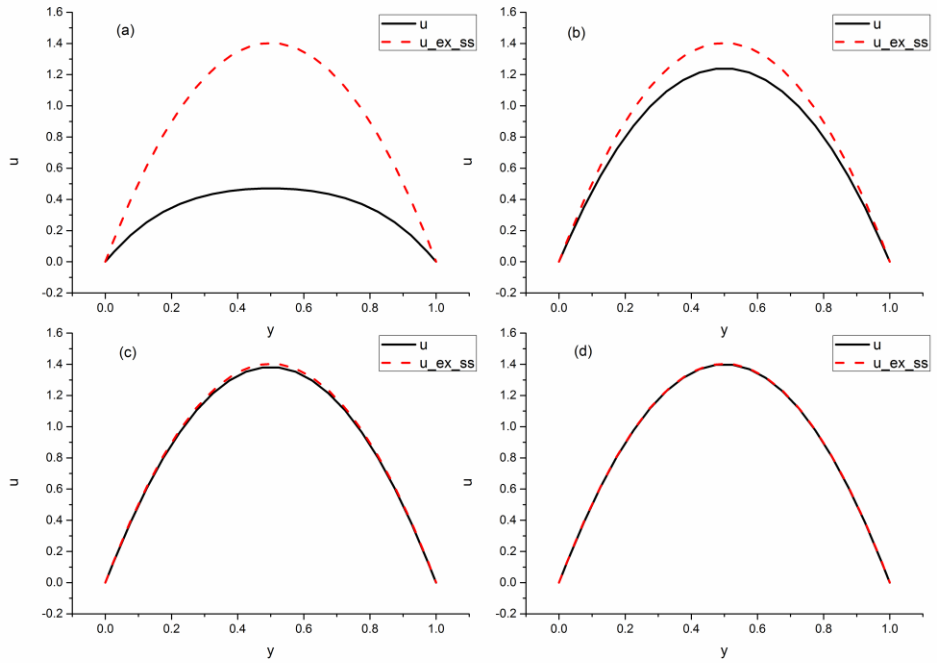

Figure 1: Distribution of velocity u and the results for the steady state given by Equation (74) for various values of t : (a) $t=0.5$; (b) $t=2.5$; (c) $t=5$; (d) $t=15$.

7.2. Applications to 2D flows

If we assume in 2D problems

$$\sigma = 0 \ \text{ in } V\,, \tag{75a}$$

$$\mathbf{u} = 0 \ \text{ on } S \tag{75b}$$

and substitute

$$\mathbf{u} = u\mathbf{e}_1 + v\mathbf{e}_2\,,\ \boldsymbol{\omega} = \omega\mathbf{e}_3\,, \tag{76a}$$

$$\mathbf{x} = x\mathbf{e}_1 + y\mathbf{e}_2\,,\ \boldsymbol{\xi} = \xi\mathbf{e}_1 + \eta\mathbf{e}_2\,, \tag{76b}$$

$$\mathbf{n}_\xi = n_{\xi 1}\mathbf{e}_1 + n_{\xi 2}\mathbf{e}_2\,, \tag{76c}$$

$$\mathbf{u}_\infty = u_\infty \mathbf{e}_1 \tag{76d}$$

into Equations (48), (52), and (53), we obtain

$$\varepsilon u(x,y,t) = -\frac{1}{2\pi}\int_V \frac{y-\eta}{(x-\xi)^2+(y-\eta)^2}\omega(\xi,\eta,t)\,dV_\xi + u_\infty\,, \tag{77a}$$

$$\varepsilon v(x,y,t) = \frac{1}{2\pi}\int_V \frac{x-\xi}{(x-\xi)^2+(y-\eta)^2}\omega(\xi,\eta,t)\,dV_\xi\,, \tag{77b}$$

$$\begin{aligned}\varepsilon\omega(x,y,t) = {} & \frac{-1}{2\pi}\int_S \frac{(x-\xi)n_{\xi 1}+(y-\eta)n_{\xi 2}}{(x-\xi)^2+(y-\eta)^2}\omega(\xi,\eta,t)\,dS_\xi + \frac{1}{2\pi\nu}\int_S B(\xi,\eta,t)\frac{(x-\xi)n_{\xi 2}-(y-\eta)n_{\xi 1}}{(x-\xi)^2+(y-\eta)^2}\,dS_\xi \\ & + \frac{1}{2\pi\nu}\int_V \frac{\partial\omega(\xi,\eta,t)}{\partial t}\ln\left(\sqrt{(x-\xi)^2+(y-\eta)^2}\right)dV_\xi + \frac{1}{2\pi\nu}\int_V \frac{(x-\xi)}{(x-\xi)^2+(y-\eta)^2}u(\xi,\eta,t)\omega(\xi,\eta,t)\,dV_\xi \\ & + \frac{1}{2\pi\nu}\int_V \frac{(y-\eta)}{(x-\xi)^2+(y-\eta)^2}v(\xi,\eta,t)\omega(\xi,\eta,t)\,dV_\xi\,,\end{aligned} \tag{78}$$

$$\varepsilon B(x,y,t) - \frac{1}{2\pi}\int_S B(\xi,\eta,t)\frac{\partial\ln\left(\sqrt{(x-\xi)^2+(y-\eta)^2}\right)}{\partial n_\xi}\,dS_\xi = -\frac{1}{2\pi}\int_S \nu\frac{[(x-\xi)n_{\xi 2}-(y-\eta)n_{\xi 1}]}{(x-\xi)^2+(y-\eta)^2}\omega(\xi,\eta,t)dS_\xi$$

$$+\frac{1}{2\pi}\int_V \frac{(x-\xi)}{(x-\xi)^2+(y-\eta)^2} v(\xi,\eta,t)\omega(\xi,\eta,t)\,dV_\xi - \frac{1}{2\pi}\int_V \frac{(y-\eta)}{(x-\xi)^2+(y-\eta)^2} u(\xi,\eta,t)\omega(\xi,\eta,t)dV_\xi \,. \tag{79}$$

7.2.1. Flow around a circular cylinder.

We assume that the center of a circular cylinder of radius R is located at the origin of the coordinates. We define the cylindrical coordinates (r,θ) as follows:

$$x=-r\cos\theta\,,\ \ y=r\sin\theta\,, \tag{80}$$

where $\theta=0$ coincides with $y=0, x<0$. This definition is convenient when the uniform flow directs to the positive $x-$axis. For simplicity, we define the computational fluid region V by

$$R\le r\le R_0\,,\ \ 0\le\theta\le 2\pi\,. \tag{81}$$

$r=R_0$ is the virtual infinite-far boundary. We use

$$\xi=-\rho\cos\phi\,,\ \ \eta=\rho\sin\phi \tag{82}$$

and

$$n_{\xi 1}=\cos\phi\,,\ \ n_{\xi 2}=-\sin\phi\,. \tag{83}$$

Next, we discretize the integral representations given by Equations (77) through (79). For simplicity, we divide the circumferential and radial directions equally. In other words, the calculation region is divided into $M\times N$ elements defined by $\theta_i-d\theta/2<\theta<\theta_i+d\theta/2$, $r_j-dr/2<r<r_j+dr/2$, $i=0,1,\cdots,M-1$, and $j=0,1,\cdots,N-1$, where $d\theta$, dr, θ_i, and r_j are defined as follows:

$$d\theta=\frac{2\pi}{M}\,,\ \ dr=\frac{R_0-R}{N}\,, \tag{84}$$

$$\theta_i=(i+0.5)d\theta\,,\ \ i=0,1,\cdots,M-1\,, \tag{85a}$$

$$r_j=R+(j+0.5)dr\,,\ \ j=0,1,\cdots,N-1\,. \tag{85b}$$

The center of the element (x_{ij},y_{ij}) are given by

$$x_{ij}=-r_j\cos\theta_i\,,\ \ y_{ij}=r_j\sin\theta_i\,. \tag{86}$$

We discretize the integral representations given by Equations (77) through (79) using Equations (84) through (86) as

$$\varepsilon u(x,y,t)=-\frac{1}{2\pi}\sum_{m=0}^{M-1}\sum_{n=0}^{N-1}\int_{r_n-dr/2}^{r_n+dr/2}\int_{\theta_m-d\theta/2}^{\theta_m+d\theta/2}\frac{y-\eta}{(x-\xi)^2+(y-\eta)^2}\rho d\rho d\phi\,\omega(x_{mn},y_{mn},t)+u_\infty\,, \tag{87a}$$

$$\varepsilon v(x,y,t)=\frac{1}{2\pi}\sum_{m=0}^{M-1}\sum_{n=0}^{N-1}\int_{r_n-dr/2}^{r_n+dr/2}\int_{\theta_m-d\theta/2}^{\theta_m+d\theta/2}\frac{x-\xi}{(x-\xi)^2+(y-\eta)^2}\rho d\rho d\phi\,\omega(x_{mn},y_{mn},t)\,, \tag{87b}$$

$$\begin{aligned}\varepsilon\omega(x,y,t)=&\frac{-1}{2\pi}\sum_{m=0}^{M-1}\int_{\theta_m-d\theta/2}^{\theta_m+d\theta/2}\frac{(x-\xi)\cos\phi-(y-\eta)\sin\phi}{(x-\xi)^2+(y-\eta)^2}Rd\phi\,\omega(-R\cos\theta_m,R\sin\theta_m,t)\\&-\frac{1}{2\pi\nu}\sum_{m=0}^{M-1}\int_{\theta_m-d\theta/2}^{\theta_m+d\theta/2}\frac{(x-\xi)\sin\phi+(y-\eta)\cos\phi}{(x-\xi)^2+(y-\eta)^2}Rd\phi\,B(-R\cos\theta_m,R\sin\theta_m,t)\\&+\frac{1}{2\pi\nu}\sum_{m=0}^{M-1}\sum_{n=0}^{N-1}\int_{r_n-dr/2}^{r_n+dr/2}\int_{\theta_m-d\theta/2}^{\theta_m+d\theta/2}\ln\left(\sqrt{(x-\xi)^2+(y-\eta)^2}\right)\rho d\rho d\phi\frac{\partial\omega(x_{mn},y_{mn},t)}{\partial t}\\&+\frac{1}{2\pi\nu}\sum_{m=0}^{M-1}\sum_{n=0}^{N-1}\int_{r_n-dr/2}^{r_n+dr/2}\int_{\theta_m-d\theta/2}^{\theta_m+d\theta/2}\frac{(x-\xi)}{(x-\xi)^2+(y-\eta)^2}\rho d\rho d\phi\,u(x_{mn},y_{mn},t)\omega(x_{mn},y_{mn},t)\\&+\frac{1}{2\pi\nu}\sum_{m=0}^{M-1}\sum_{n=0}^{N-1}\int_{r_n-dr/2}^{r_n+dr/2}\int_{\theta_m-d\theta/2}^{\theta_m+d\theta/2}\frac{(y-\eta)}{(x-\xi)^2+(y-\eta)^2}\rho d\rho d\phi\,v(x_{mn},y_{mn},t)\omega(x_{mn},y_{mn},t)\,,\end{aligned} \tag{88}$$

$$\begin{aligned}&\varepsilon B(x,y,t)+\frac{1}{2\pi}\sum_{m=0}^{M-1}\int_{\theta_m-d\theta/2}^{\theta_m+d\theta/2}\frac{(x-\xi)\cos\phi-(y-\eta)\sin\phi}{(x-\xi)^2+(y-\eta)^2}Rd\phi\,B(-R\cos\theta_m,R\sin\theta_m,t)\\&=\frac{\nu}{2\pi}\sum_{m=0}^{M-1}\int_{\theta_m-d\theta/2}^{\theta_m+d\theta/2}\frac{(x-\xi)\sin\phi+(y-\eta)\cos\phi}{(x-\xi)^2+(y-\eta)^2}Rd\phi\,\omega(-R\cos\theta_m,R\sin\theta_m,t)\\&+\frac{1}{2\pi}\sum_{m=0}^{M-1}\sum_{n=0}^{N-1}\int_{r_n-dr/2}^{r_n+dr/2}\int_{\theta_m-d\theta/2}^{\theta_m+d\theta/2}\frac{(x-\xi)}{(x-\xi)^2+(y-\eta)^2}\rho d\rho d\phi\,v(x_{mn},y_{mn},t)\omega(x_{mn},y_{mn},t)\\&-\frac{1}{2\pi}\sum_{m=0}^{M-1}\sum_{n=0}^{N-1}\int_{r_n-dr/2}^{r_n+dr/2}\int_{\theta_m-d\theta/2}^{\theta_m+d\theta/2}\frac{(y-\eta)}{(x-\xi)^2+(y-\eta)^2}\rho d\rho d\phi\,u(x_{mn},y_{mn},t)\omega(x_{mn},y_{mn},t)\,.\end{aligned} \tag{89}$$

If we consider the integral representation given by Equation (89) of B on the surface of the cylinder, the integral representation is an integral equation with respect to $B(-R\cos\theta, R\sin\theta, t)$. However, caution is required, because the equation is a singular integral equation. We can solve the equation using the property of the kernel function:

$$\frac{(x-\xi)\cos\phi-(y-\eta)\sin\phi}{(x-\xi)^2+(y-\eta)^2}=\frac{-R(\cos\theta-\cos\phi)\cos\phi-R(\sin\theta-\sin\phi)\sin\phi}{R^2(\cos\theta-\cos\phi)^2+R^2(\sin\theta-\sin\phi)^2}=\frac{1}{R}\,\frac{-\cos(\theta-\phi)+1}{2-2\cos(\theta-\phi)}=\frac{1}{2R}, \tag{90}$$

If we denote the right-hand side of Equation (89) as $f(x,y,t)$, then Equation (89) becomes on the surface of the cylinder

$$B(-R\cos\phi,R\sin\phi,t)+\overline{B(-R\cos\phi,R\sin\phi,t)}=2f(-R\cos\phi,R\sin\phi,t). \tag{91}$$

Taking the average with respect to ϕ, we have

$$\overline{B(-R\cos\phi,R\sin\phi,t)}=\overline{f(-R\cos\phi,R\sin\phi,t)}. \tag{92}$$

We then obtain

$$B(-R\cos\phi,R\sin\phi,t)=2f(-R\cos\phi,R\sin\phi,t)-\overline{f(-R\cos\phi,R\sin\phi,t)}. \tag{93}$$

Next, we present an algorithm for the numerical calculation. Using Solution A1.2 with the integral representations given by Equations (87) through (89):

(1) Assume $\boldsymbol{\omega}(\mathbf{x},t)$ on IP at time t.

(2) Obtain $\mathbf{u}(\mathbf{x},t)$ on IP and BP using Equation (87).

(3) Solve the boundary integral equation given by Equation (89) for $B(\mathbf{x},t)$ on BP.

(4) Solve the integral equation given by Equation (88) for $\partial\boldsymbol{\omega}(\mathbf{x},t)/\partial t$ on IP and $\boldsymbol{\omega}(\mathbf{x},t)$ on BP.

(5) Obtain $\boldsymbol{\omega}(\mathbf{x},t+dt)$ from $\boldsymbol{\omega}(\mathbf{x},t+dt)=\boldsymbol{\omega}(\mathbf{x},t)+(\partial\boldsymbol{\omega}(\mathbf{x},t)/\partial t)dt$.

(6) Make the time $t+dt$ and repeat the process.

In Step (1), $\boldsymbol{\omega}(\mathbf{x},t)$ is known at $t=0$ from the initial condition. In Step (2), $\mathbf{u}(\mathbf{x},t)$ is obtained by evaluating the integral on the right-hand side of Equation (87). In step (3), if we substitute $\mathbf{u}(\mathbf{x},t)$ and $\boldsymbol{\omega}(\mathbf{x},t)$ on the right-hand side of Equation (89) and consider on BP, Equation (89) is an integral equation for the unknown $B(\mathbf{x},t)$. If we consider Equation (88) on IP and BP, then Equation (88) is an integral equation for the unknowns $\partial\boldsymbol{\omega}(\mathbf{x},t)/\partial t$ on IP and $\boldsymbol{\omega}(\mathbf{x},t)$ on BP. In step (4), we solve the integral equation for the unknowns $\partial\boldsymbol{\omega}(\mathbf{x},t)/\partial t$ on IP and $\boldsymbol{\omega}(\mathbf{x},t)$ on BP. In step (5), we obtain $\boldsymbol{\omega}(\mathbf{x},t+dt)$ on IP. At every time step, we can calculate the slip of the tangential velocity on the surface of the cylinder using the difference of the tangential component of $\mathbf{u}(\mathbf{x},t)$ obtained by Equation (87) and that obtained by the boundary condition. We must adjust the vorticity in the elements adjacent to the surface of the cylinder using Equation (100).

Numerical calculations are conducted by using the discretized equations given by Equation (87) through (89). We must evaluate the integrals on the right-hand side of these equations numerically. For example, the integrals on the right-hand side of Equation (87) are calculated as follows. We divide an element into $M_1\times N_1$ sub-elements as

$$d\theta_1=\frac{d\theta}{M_1},\ dr_1=\frac{dr}{N_1}, \tag{94a}$$

$$\theta_{1m_1}=\theta_m-0.5d\theta+(m_1+0.5)d\theta_1,\ r_{1n_1}=\theta_n-0.5d\theta+(n_1+0.5)dr_1, \tag{94b}$$

$$x_{1m_1n_1}=-Rr_{1n_1}\cos\theta_{1m_1},\ y_{1m_1n_1}=Rr_{1n_1}\sin\theta_{1m_1n_1} \tag{94c}$$

and approximate the integrals as

$$\int_{r_n-dr/2}^{r_n+dr/2}\int_{\theta_m-d\theta/2}^{\theta_m+d\theta/2}\frac{x-\xi}{(x-\xi)^2+(y-\eta)^2}\rho\,d\rho\,d\phi=\sum_{m_1=0}^{M_1-1}\sum_{n_1=0}^{N_1-1}\frac{x-x_{1m_1n_1}}{(x-x_{1m_1n_1})^2+(y-y_{1m_1n_1})^2}r_n\,dr_1\,d\theta_1, \tag{95a}$$

$$\int_{r_n-dr/2}^{r_n+dr/2}\int_{\theta_m-d\theta/2}^{\theta_m+d\theta/2}\frac{y-\eta}{(x-\xi)^2+(y-\eta)^2}\rho\,d\rho\,d\phi=\sum_{m_1=0}^{M_1-1}\sum_{n_1=0}^{N_1-1}\frac{y-y_{1m_1n_1}}{(x-x_{1m_1n_1})^2+(y-y_{1m_1n_1})^2}r_n\,dr_1\,d\theta_1. \tag{95b}$$

The pressure p is obtained using Equation (6). In other words, for the pressure p and the pressure coefficient C_p, we use

$$p-p_\infty=\rho\left[B-\frac{1}{2}(\mathbf{u}\cdot\mathbf{u}-\mathbf{u}_\infty\cdot\mathbf{u}_\infty)\right], \tag{96a}$$

$$C_p=\frac{(p-p_\infty)}{\frac{1}{2}\rho u_\infty^2}. \tag{96b}$$

The frictional stress τ and the coefficient of friction C_f on the surface of the cylinder are calculated as

$$\tau = \mu\left[\frac{\partial u_\theta}{\partial r}\right]_{r=R} = -\mu\omega(R,\theta,t)\,, \tag{97a}$$

$$C_f = \frac{\tau}{\frac{1}{2}\rho u_\infty^2}\,. \tag{97b}$$

The pressure drag D_p, friction drag D_f, and total drag D_t are obtained as

$$D_p = \int_0^{2\pi} p\cos\theta R d\theta\,,\ D_f = \int_0^{2\pi} \tau\sin\theta R d\theta\,,\ D_t = D_p + D_f\,, \tag{98a}$$

and the pressure drag coefficient C_{Dp}, friction drag coefficient C_{Df}, and total drag coefficient C_{Dt} are obtained as

$$C_{Dp} = \frac{D_p}{\frac{1}{2}\rho u_\infty^2 2R}\,,\ C_{Df} = \frac{D_f}{\frac{1}{2}\rho u_\infty^2 2R}\,,\ C_{Dt} = C_{Dp} + C_{Df}\,. \tag{98b}$$

The pressure lift L_p, friction lift L_f, and total lift L_t are obtained by

$$L_p = -\int_0^{2\pi} p\sin\theta R d\theta\,,\ L_f = \int_0^{2\pi} \tau\cos\theta R d\theta\,,\ L_t = L_p + L_f\,, \tag{99a}$$

and the pressure lift coefficient C_{Lp}, friction lift coefficient C_{Lf} and total lift coefficient C_{Lt} are obtained as

$$C_{Lp} = \frac{L_p}{\frac{1}{2}\rho u_\infty^2 2R}\,,\ C_{Lf} = \frac{L_f}{\frac{1}{2}\rho u_\infty^2 2R}\,,\ C_{Lt} = C_{Lp} + C_{Lf}\,. \tag{99b}$$

A. Case in which no Karman vortex train exists

In the following calculations, we specify $u_\infty = U = 1$ at $t = 0$ and keep the condition. Hence, slip occurs on the surface of the cylinder at $t = 0$. We calculate the vorticity due to the slip and add to the vorticity in the elements adjacent to the surface of the cylinder. The slip due to the error of the calculations is also treated similarly. Namely, we add $\Delta\omega$ given by

$$\Delta\omega(R + dr/2,\theta,t) = -\frac{u_\theta(R,\theta,t)}{dt} \tag{100}$$

to the vorticity in the elements adjacent to the surface of the cylinder. We use $R = 0.5$, $\rho = 1000$, $M_1 = 2$ and $N_1 = 2$.

First, we present the case in which $\nu = 0.1$. The Reynolds number R_n :

$$R_n = \frac{2RU}{\nu} \tag{101}$$

is 10. We assume that $R_0 = 8$, $M = 40$, $N = 20$, $dt = 0.01$, $dr_0 = 0.125$ (Courant number in the radial direction: $C_{Nr} = Udt/dr_0 = 0.08$), and $dr_{N-1} = 0.75$. We used an unequal division in the radial direction. Figure 2 shows the radial division. We followed Vinokur's method [9] for the unequal division.

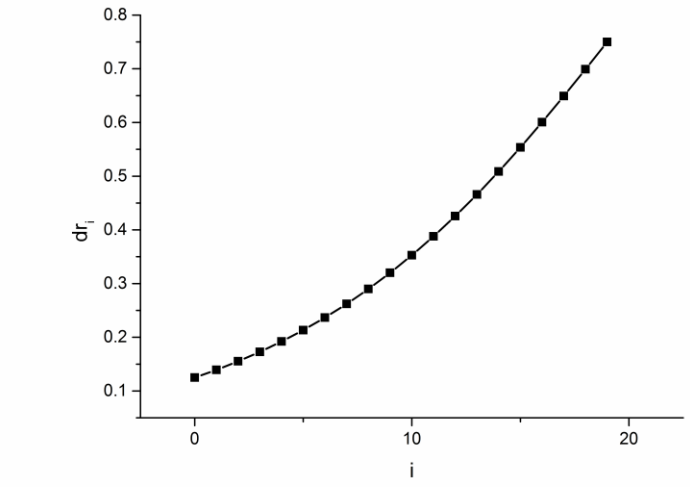

Figure 2: Distribution of element size dr_i in the radial direction.

First, we verified the convergence of the calculation conducting a calculation with a number of total time steps (*NTS*) of 3200. In Figure 3, we show the convergence of the integral of the vorticity in the upper half space

$\int_R^{R_0}\int_0^{\pi}\omega(r,\theta)rdrd\theta$, that in the lower half space $\int_R^{R_0}\int_{\pi}^{2\pi}\omega(r,\theta)rdrd\theta$ and that in the whole space $\int_R^{R_0}\int_0^{2\pi}\omega(r,\theta)rdrd\theta$, and the pressure drag coefficient C_{Dp}, friction drag coefficient C_{Df}, and total drag coefficient C_{Dt}, when $t\to\infty$. The convergence appears to be satisfactory.

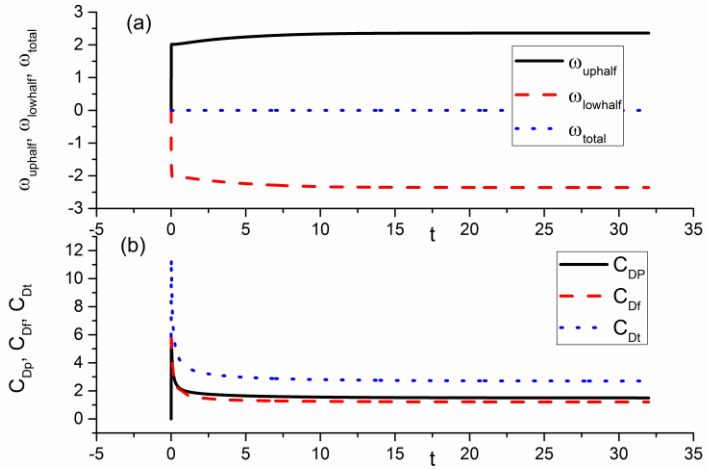

Figure 3: Convergence of solution as $t\to\infty$: (a) Vorticity integrals $\int_R^{R_0}\int_0^{\pi}\omega(r,\theta)rdrd\theta$, $\int_R^{R_0}\int_{\pi}^{2\pi}\omega(r,\theta)rdrd\theta$ and $\int_R^{R_0}\int_0^{2\pi}\omega(r,\theta)rdrd\theta$; (b) Drag coefficients C_{Dp}, C_{Df} and C_{Dt}.

The effect of the radial mesh size dr or the Courant number $C_{Nr}=Udt/dr_0$ on the numerical results is significant.

Table 1: Effects of radial mesh size dr or the Courant number $C_{Nr}=Udt/dr_0$ on the numerical results ($NTS=1600$ or $t=16$).

R_0	dr_0	dr_{19}	$C_{Nr}=\frac{u_\infty dt}{dr_0}$	C_{Dp}	C_{Df}	C_{Dt}
8	0.1667	0. 75	0.06	1.501	1.220	2.720
8	0.125	0.75	0.08	1.515	1.222	2.737
8	0.1	0.75	0.10	1.523	1.224	2.747
8	0.08	0.75	0.125	1.529	1.228	2.756
8	0.0667	0.75	0.15	1.532	1.231	2.763
8	0.125	0.5	0.08	1.515	1.222	2.737
8	0.125	1.0	0.08	1.515	1.221	2.736
6	0.125	0.563	0.08	1.524	1.227	2.752
10	0.125	0.938	0.08	1.512	1.220	2.732

In Figure 4, the distribution of the pressure coefficient C_p and friction coefficient C_f on the surface of the cylinder at $t=16$ for the case in which $R_0=8$, $dr_0=0.125$, and $dr_{N-1}=0.75$ are shown where C_{p_pt} refers to C_p obtained by the potential theory. Since the distributions of the pressure and friction coefficients are symmetric with respect to the $x-$axis, lift is not generated. A separation bubble is formed as time passes.

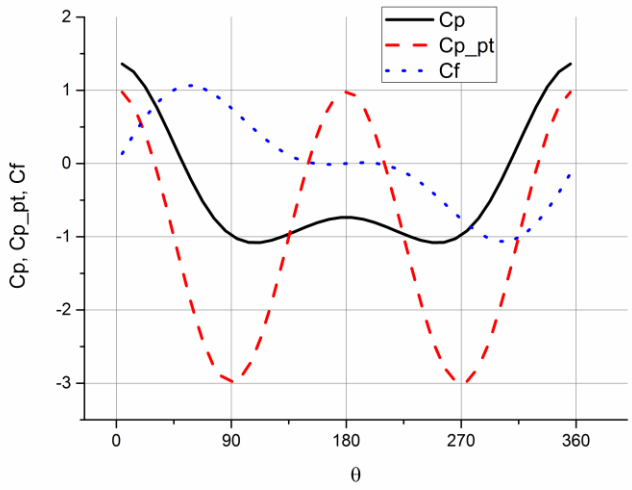

Figure 4: Distribution of the pressure coefficient C_p and the friction coefficient C_f on the surface of the cylinder ($t=16$).

When the numerical results are examined in detail for the case in which $\nu=0.05$, ω was found to be wavy in the neighborhood of the outer boundary when $150<\theta<210$. Although this appears to be a Karman vortex, since the Reynolds number $R_n=2RU/\nu$ was 20, this phenomenon cannot be Karman vortex. This indicates us that we should place the outer boundary further away. Then, we introduced a fictitious boundary condition at the outer boundary such as

$$\frac{\partial^2\omega}{\partial r^2}=0 \text{ on } r=R_0,\ \frac{\pi}{2}<\theta<\pi \tag{102}$$

and used

$$\omega_{iN-1}=2\omega_{iN-2}-\omega_{iN-3} \text{ for } M/4\le i<3M/4. \tag{103}$$

The condition given by Equation (103) corresponds to the condition given by Equation (102) when $dr_{N-1}\approx dr_{N-2}$. The numerical results were improved significantly.

Even if we introduce

$$\frac{\partial\omega}{\partial r}=0 \text{ on } r=R_0,\ \frac{\pi}{2}<\theta<\pi \tag{104}$$

on the outer boundary instead of the condition given by Equation (102) and use

$$\omega_{iN-1}=\omega_{iN-2} \text{ for } M/4\le i<3M/4, \tag{105}$$

the numerical results were similarly improved.

B. Case in which a Karman vortex train exists

We next consider the case in which the kinematic viscosity $\nu=0.01$. Since Reynolds number $R_n=2RU/\nu$ is 100, a Karman vortex is generated. Although the Karman vortex is generated naturally in numerical calculation, a significant number of time steps is required. In order to accelerate the calculation, we impose an artificial stimulus. We add the vorticity ω_{i0} $(i=0,1,\cdots,M-1)$ in the elements adjacent to the surface of the cylinder $-\alpha/M/dr_0$ during time steps 25 through 49 and $+\alpha/M/dr_0$ during time steps 50 through 74. In the following calculations, we use $\alpha=0.1$. As shown in Figure 5, we used a rectangular area following the FEM calculations by Brooks and Hughes [7] and Tezduyar, Liou and Ganjoo [8]. The center of the circular cylinder is placed at the origin of the coordinates. The radius R of the cylinder is 0.5, the width $2R_0$ of the calculation region is 16.0, the length X_W of the wake region (or the region $x>0$) is 15.5, and the length of the region R_0+X_W is 23.5. The number of the elements M in the circumferential direction is 64, the number of the elements N in the radial direction is 20, and the number of the elements N_W of the wake (or the region $R_0<x<X_W$, $-R_0<y<R_0$) in the direction of $x-$axis is 20. The radial size of the element dr_0 of the element adjacent to the surface of the cylinder is 0.06 ($C_{Nr}=Udt/dr_0=0.5$) and the radial size dr_{N-1} of the farthest elements is 0.75. The time increment dt is 0.03. Figure 5 shows the calculation region and the division into elements.

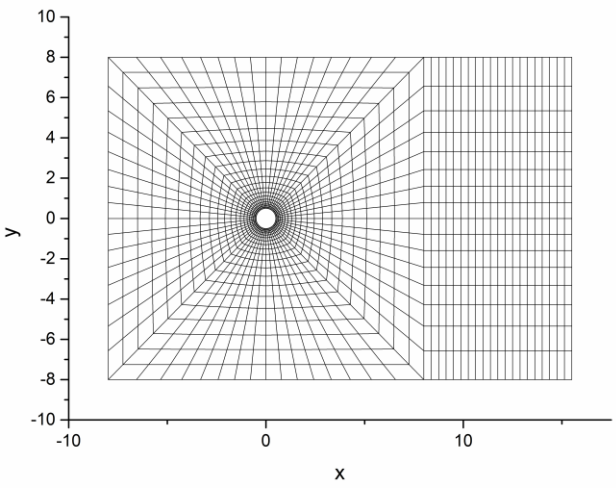

Figure 5: Calculation region and division into elements.

The vorticity integrals, drag coefficients and lift coefficients are shown in Figure 6. Since Karman vortex trains are generated in the wake, the drag and lift coefficients are oscillatory. The Strouhal number $Str = 2fR/U$ of the steady oscillation is 0.18 where f is the frequency of Karman vortex, and the variations of the total drag coefficient C_{Dt} and the total lift coefficient C_{Lt} are 1.35 to 1.38 and –0.29 to +0.29, respectively. The numerical results are close to the experimental results [10] and [11]. In these calculations, we consider a condition on the outer boundary:

$$\frac{\partial^2 \omega}{\partial x^2} = 0 \text{ on } x = X_W,\ -R_0 < y < R_0 \tag{106}$$

and impose the following condition:

$$\omega_{1,i\,N_W-1} = 2\omega_{1,i\,N_W-2} - \omega_{1,i\,N_W-3} \text{ for } 3M/8 \le i < 5M/8, \tag{107}$$

where $\omega_{1,i,j}$ is the vorticity of the element (i, j) in region 1 ($R_0 < x < X_W$, $-R_0 < y < R_0$). Furthermore, we also consider conditions:

$$\omega = 0 \text{ on } R_0 < x < X_W,\ y = \pm R_0 \tag{108}$$

and impose the following conditions:

$$\omega_{1,0,j} = 0 \text{ for } 0 \le j < N_W, \tag{109a}$$

$$\omega_{1,M/4-1,j} = 0 \text{ for } 0 \le j < N_W. \tag{109b}$$

Instead of Equations (106) and (107), we may consider the outer boundary condition:

$$\frac{\partial \omega}{\partial x} = 0 \text{ on } x = X_W,\ -R_0 < y < R_0 \tag{110}$$

and impose the following condition:

$$\omega_{1,i\,N_W-1} = \omega_{1,i\,N_W-2} \text{ for } 3M/8 \le i < 5M/8. \tag{111}$$

We obtain similar numerical results in this case.

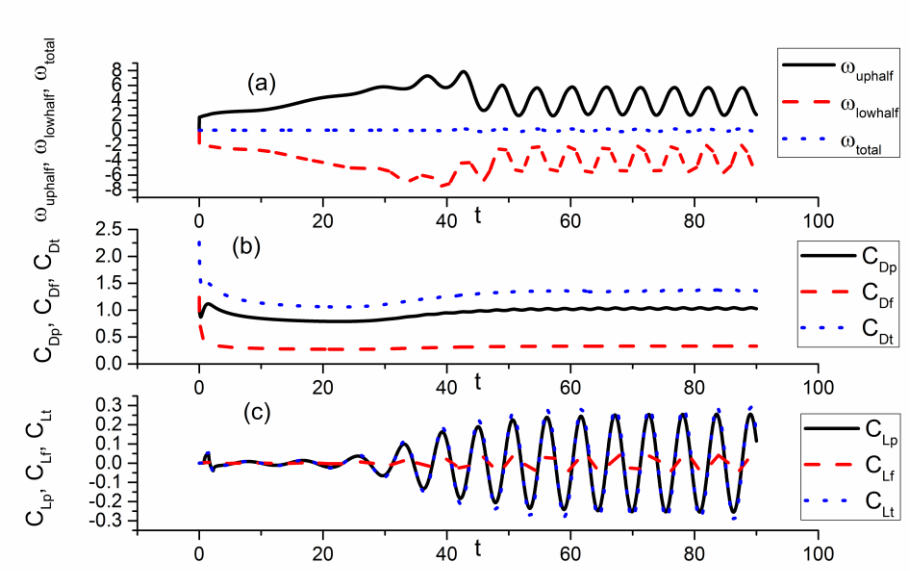

Figure 6: Change of vortex integrals, drag coefficients and lift coefficients with time: (a) Vorticity integrals $\int_R^{R_0}\int_0^{\pi}\omega(r,\theta)rdrd\theta$, $\int_R^{R_0}\int_{\pi}^{2\pi}\omega(r,\theta)rdrd\theta$ and $\int_R^{R_0}\int_0^{2\pi}\omega(r,\theta)rdrd\theta$; (b) Drag coefficients C_{Dp}, C_{Df} and C_{Dt}; (c) Lift coefficients C_{Lp}, C_{Lf} and C_{Lt}.

In Figure 7, we show the space distributions of the vorticity, pressure coefficient and velocity components at $t=90$. The solid and dashed lines mean the positive and negative values of the corresponding quantities, respectively.

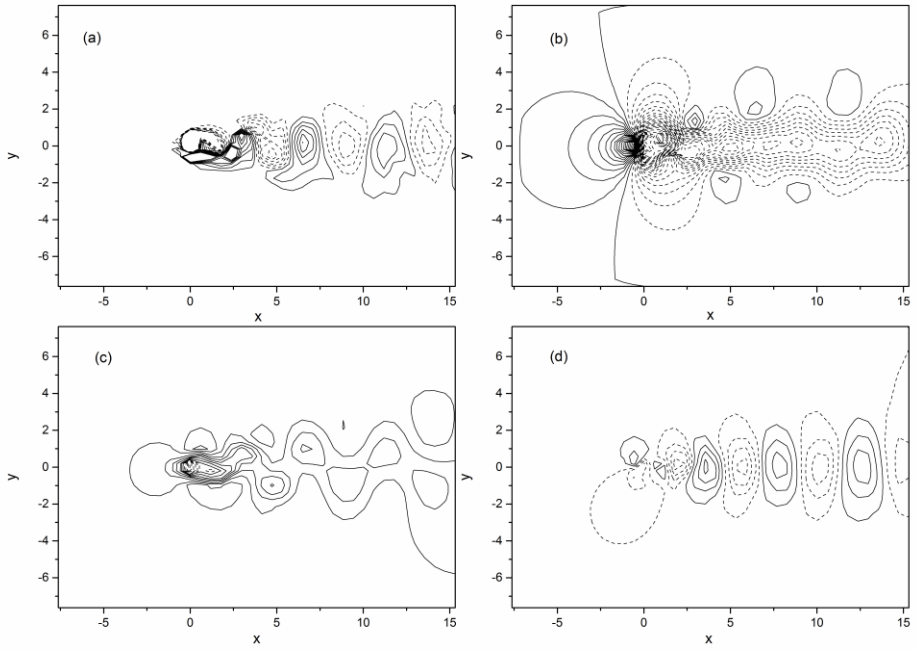

Figure 7: Space distribution of vorticity, pressure coefficient and velocity at $t=90$: (a) Vorticity ω; (b) Pressure coefficient C_p; (c) Velocity component u in the $x-$direction; (d) Velocity component v in the $y-$direction.

In the above numerical results, the number of division M in the $\theta-$direction was 64. We varied M and studied the effects. The results are shown in Figure 8. If we increase M, then C_{Dt}, C_{Lt}, and Str converge to constant values. We

examined the boundary condition on the surface of the cylinder and found that the satisfaction of the boundary condition was improved better when M is increased.

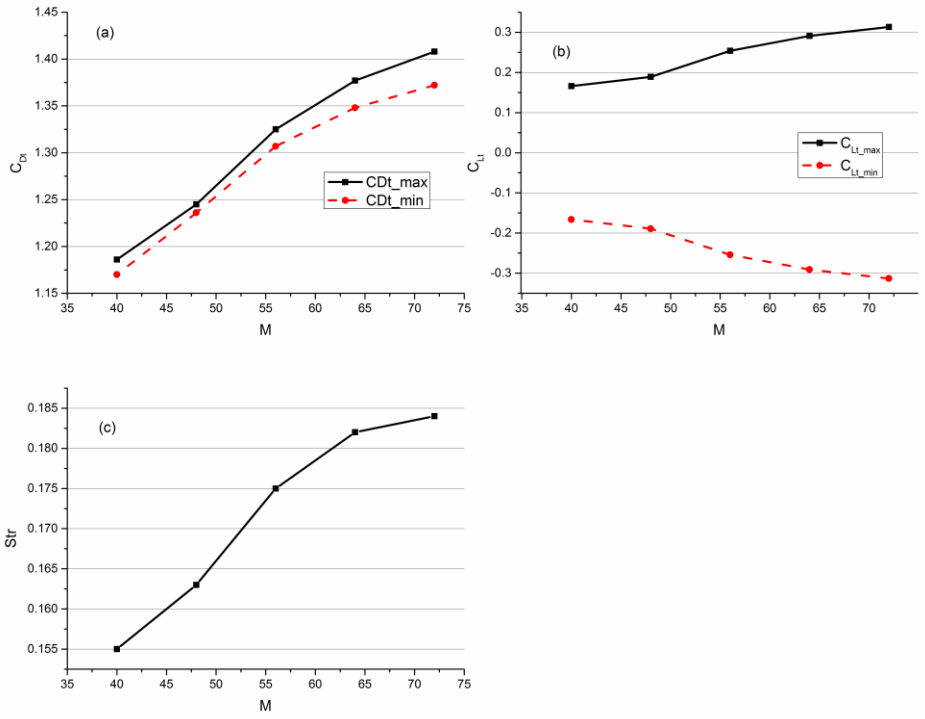

Figure 8: Effect of division number M in the $\theta-$direction on the total drag coefficient, total lift coefficient, and Strouhal number: (a) Total drag coefficient C_{Dt}; (b) Total lift coefficient C_{Lt}; (c) Strouhal number Str.

In the following, the computational results are compared with the experimental ones. Figure 9 shows a comparison of the calculated pressure coefficient C_p with the experimental one by Grove et al. [10] at $R_n = 40$. The calculation conditions are as follows: $R_0 = 8$, $R = 0.5$, $M = 64$, $N = 20$, $dr_0 = 0.05$, $dr_{N-1} = 0.75$, $N_W = 20$, $X_W = 15.5$, $dx_W = 0.375$, $\rho = 1000$, $\nu = 0.025$, $dt = 0.025$, and $NTS = 2000$. The Reynolds number $Rn = 2UR/\nu$, Courant number in the $r-$direction $C_{Nr} = Udt/dr_0$, and Courant number in the $r-$direction $C_{N\theta} = Udt/(Rd\theta)$ are 40, 0.5093, and 0.5, respectively. The calculated C_p appears to be appropriate.

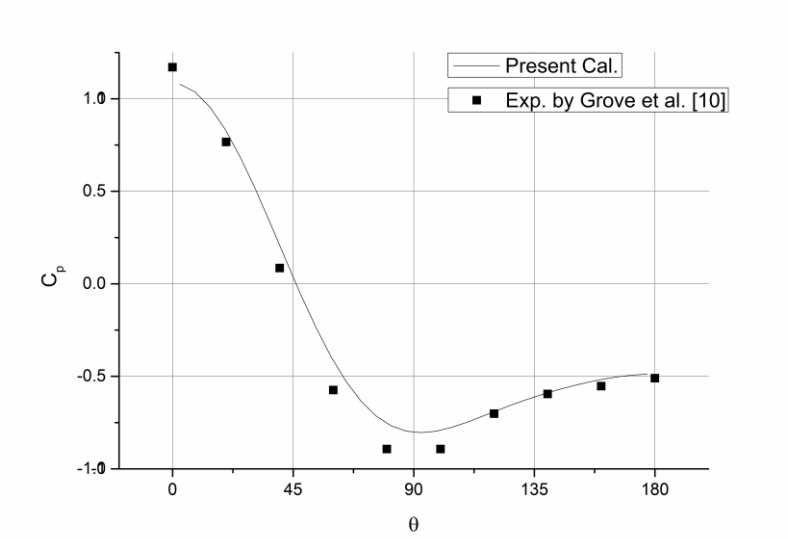

Figure 9: Pressure coefficient C_p on surface of cylinder at $R_D = 40$ ($t = 50$).

In Figure 10, the calculated total drag coefficient C_{Dt} is compared with the experimental one [11] with the various Reynolds number R_n. The comparison of C_{Dt} between the calculation and the experiment appears to be appropriate. The calculation conditions are presented in Table 2. The time in which C_{Dt} is calculated is equal to $TNS \times dt$ in Table 2. C and R in the table refer to the circular and rectangular regions used in the calculations.

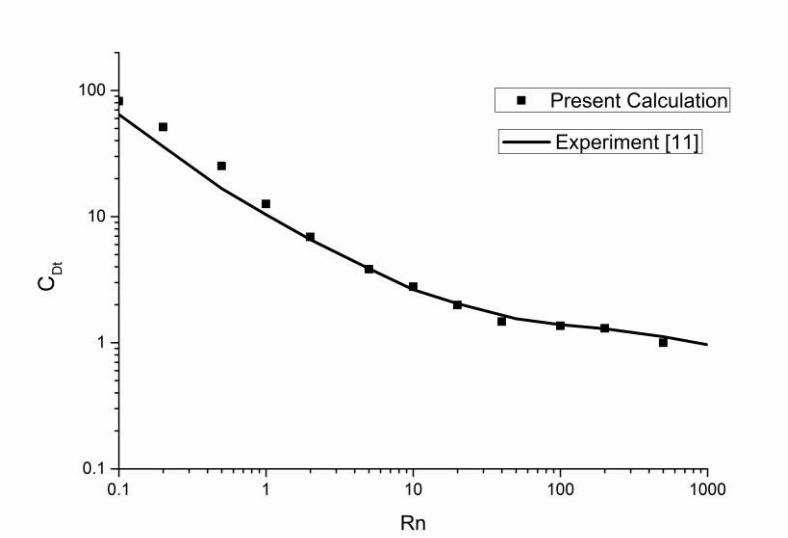

Figure 10: The comparison of C_{Dt} between the calculation and the experiment with various Reynolds number R_n.

Table 2: The calculation conditions for the numerical results in Figure 10.

	#1	#2	#3	#4	#5	#6	#7	#8	#9	#10	#11	#12	#13
R_n	0.1	0.2	0.5	1	2	5	10	20	40	40	100	200	500
C_{Dt}	82.2	51.3	25.2	12.6	6.90	3.83	2.78	1.99	1.47	1.47	1.36	1.3	0.80
R	0.5	0.5	0.5	0.5	0.5	0.5	0.5	0.5	0.5	0.5	0.5	0.5	0.5
U	1.0	1.0	1.0	1.0	1.0	1.0	1.0	1.0	1.0	1.0	1.0	1.0	1.0
ν	10.0	5.0	2.0	1.0	0.5	0.2	0.1	0.05	0.025	0.025	0.01	0.005	0.002
Reg.	C	C	C	C	C	C	C	C	C	R	R	R	R
R_0	16.0	16.0	8.0	8.0	8.0	8.0	8.0	8.0	8.0	8.0	8.0	8.0	6.0
M	16	16	16	24	24	24	32	32	32	64	64	64	64
N	10	10	10	10	16	16	16	16	16	20	20	20	20
X_w										15.5	15.5	23	23
N_w										20	20	20	20
dr_0	0.7	0.35	0.35	0.35	0.35	0.35	0.125	0.125	0.125	0.05	0.06	0.06	0.06
$10^3 C_{Nr}$	0.22	0.45	0.45	3.57	7.14	14.3	80	80	80	500	500	250	125
$10^3 C_{N\theta}$	0.8	0.8	0.8	9.6	19.1	38.2	101.9	101.9	101.9	509	611.2	305.6	152.8
dr_{N-1}	2.0	2.0	2.0	1.0	1.0	1.0	0.75	0.75	0.75	0.75	0.75	0.75	0.75
$10^3 dt$	0.16	0.16	0.16	1.25	2.5	5	10	10	10	25	30	15	7.5
α	0	0	0	0	0	0	0	0	0	0	0.1	0.05	0.025
$\frac{TNS}{1000}$	8.55	6	6	3	3	2	1.6	1.6	1.6	2	3	6	12

In Figure 11, the very interesting change of the pressure coefficient C_p and the friction coefficient C_f on the surface of the cylinder with the change of the Reynolds number is shown. In the figure, C_{p_pt} refers to C_p obtained by the potential theory. The time in which C_p and C_f are calculated is equal to $TNS \times dt$ in Table 2.

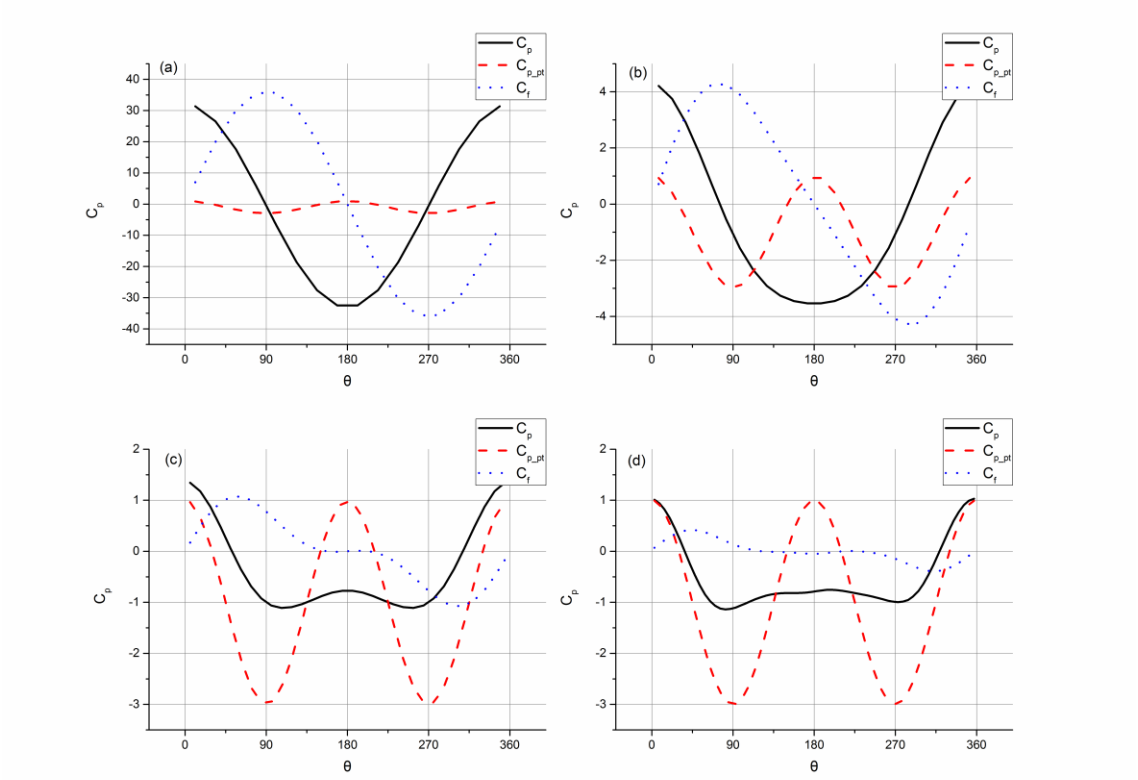

Figure 11: Change of pressure coefficient C_p and friction coefficient C_f with the Reynolds number R_n: (a) $R_n = 0.1$; (b) $R_n = 1$; (c) $R_n = 10$; (d) $R_n = 100$.

8. CONCLUSIONS

A set of integral representations is obtained using a fundamental solution of a differential-type boundary value problem. Unknown variables of the boundary value problem can be determined solving a set of integral equations derived from the set of integral representations. In the present paper, a boundary value problem expressed by a set of integral representations is referred to as an integral-type boundary value problem. Two types of numerical calculations were considered, 1D and 2D problems. Hagen-Poiseuille flows were discussed as 1D problems and revealed the basic aspects of the integral representation method. Numerical calculations of laminar viscous flows around a circular cylinder in a uniform flow were examined as 2D problems, and the obtained results were appropriate in comparison with experiments. Important characteristics of the integral representation method (IRM) were clarified through the calculations.

By using the IRM, more precise calculation results may be obtained by using a narrower calculation region and a coarser mesh division. This was confirmed by the numerical calculations discussed herein.

Unlike FEM, as seen from that constant distribution of the unknown variables is possible, IRM may not assume the continuity of the unknown variables between elements from the beginning. It would be safe to say this is a big advantage of IRM. In the case of IRM, a higher-order distribution may be introduced easily. By introducing the implicit method in time progression, a drastic improvement of the accuracy, stability and computational efficiency could be expected.

9. REFERENCES

[1] J.C. Wu, J.F. Thompson, "Numerical solutions of time-dependent incompressible Navier-Stokes equations using an integro-differential formulations", *Computers & Fluids*, (1973), **1,** pp. 197-215.

[2] J.C. Wu, "Chap. 4 Problems of general viscous flow", *Developments in Boundary Element Methods-2, edited by P. K. Banerjee and R. P. Shaw*, Applied Science Publishers, (1982), pp. 69-109.

[3] J.C. Wu, "Fundamental solutions and boundary element method", *Engineering Analysis*, (1987), **4(**1), pp. 2-6.

[4] J.C. Wu, C.M. Wang, "Chap. 7 Recent advances in solution methods for unsteady viscous flows", *Boundary Element Methods in Nonlinear Fluid Dynamics, Developments in Boundary Element Methods-6, edited by P. K. Banerjee and L. Morino*, Elsvier Applied Science, (1990), 247-283.

[5] J.S. Uhlman, "An integral equation formulation of the equations of motion of an incompressible fluid", *NUWC-NPT Technical Report 10,086, 15 July*, (1992).

[6] A.J. Chorin, "Numerical study of slightly viscous flow", *J, Fuid Mech.*, (1973), **57**, pp. 785-796.

[7] A.N. Brooks, T.R. Hughes, "Streamline Upwind/Petrov-Galerkin formulations for Convection dominated Flows with particular emphasis on the incompressible Navier-Stokes equations", *Computer Methods in Applied Mechanics and Engineering*, (1982), **32**, pp. 199-259.
[8] T.E. Tezduyar, J. Liou, D.K. Ganjoo, "Incompressible flow computations based on the vorticity-stream function and velocity-pressure formulations, *Computers &* Structures", (1990), **35(**4), pp. 445-472.
[9] M. Vinokur, "On one-dimensional stretching functions for finite-difference calculations", *NASA Contractor Report 3313*, (1980).
[10] A.S. Grove, F.H. Shair, E.E. Petersen, A. Acrivos, "An experimengtal investigation of the steady separated flow past a circular cylinder", *J. Fluid Mech*., (1964), **33**, 60-80 .
[11] J.D. Anderson, Fundamentals of Aerodynamics, *4th ed*. McGraw-Hill, (2005), pp.228–236.
[12] C.Y. Choi, E. Balaras, "A dual reciprocity boundary element formulation using the fractional step method for the incompressible navier-Stokes equations", Engineering Analysis with Boundary Elements **33**(6), June 2009, Pages 741–749
[13] J. Matsunashi, N. Okamoto, T. Futagami, "Boundary element analysis of Navier-Stokes equations", Engineering Analysis with Boundary Elements, (2012), 36, pp.471-476.
[14] G.B.L. Ying, D. Zorin, "The embedded boundary integral method (EBI) for the incompressible Navier-Stokes equations, UT Austin, TX, USA, May 28-30, (2002), pp. 1-12.
[15] N. Tosaka, K. Onishi, "Boundary integral equation formulations for steady Navier-Stokes equations using the Stokes-fundamental solutions", Engineering Analysis, (1985), **2**(3), pp. 128-132.

10. LIST OF SYMBOLS

ρ : density of fluid
ν : kinematic viscosity of fluid
$\mathbf{e}_1$, $\mathbf{e}_2$ and $\mathbf{e}_3$: base vectors of Cartesian coordinates in the fluid region
V : fluid region
t : time
$\mathbf{x} = x_i\mathbf{e}_i = x_1\mathbf{e}_1 + x_2\mathbf{e}_2 + x_3\mathbf{e}_3 = (x, y, z)$: position vector
$\boldsymbol{\xi} = \xi_i\mathbf{e}_i = \xi_1\mathbf{e}_1 + \xi_2\mathbf{e}_2 + \xi_3\mathbf{e}_3 = (\xi, \eta, \xi)$: position vector
$\mathbf{u}(\mathbf{x},t) = u_i(\mathbf{x},t)\mathbf{e}_i = u_1\mathbf{e}_1 + u_2\mathbf{e}_2 + u_3\mathbf{e}_3 = (u, v, w)$: velocity vector
$p(\mathbf{x},t)$: pressure
$\nabla = \mathbf{e}_i\,\partial/\partial x_i$: nabla operator
σ : source of fluid per unit volume
$\boldsymbol{\omega}$: vorticity
B : total pressure
p_∞ : pressure at infinity
S : body surface
$\mathbf{u}_B$: fluid velocity on body surface
$\mathbf{n}$: unit outward normal of the boundary surface
$\phi(\mathbf{x})$: velocity potential
$G(\mathbf{x},\boldsymbol{\xi})$: fundamental solution of Laplace operator
$\boldsymbol{\xi} = \xi_i\mathbf{e}_i = \xi_1\mathbf{e}_1 + \xi_2\mathbf{e}_2 + \xi_3\mathbf{e}_3 = (\xi, \eta, \xi)$: position vector
$\Delta_{\mathbf{x}} = \nabla^2_{\mathbf{x}} = \partial^2/\partial x_i\partial x_i$: Laplace operator
$\delta(\mathbf{x},\boldsymbol{\xi})$: Dirac's delta function
$\varepsilon(\mathbf{x})$: function befined by Equation (17)
$r(\mathbf{x},\boldsymbol{\xi}) = |\,\mathbf{x} - \boldsymbol{\xi}\,|$: radial distance
S_∞ : infinite boundary
$\mathbf{u}_\infty$: uniform flow
A : defined by Equation (49)
C : defined by Equation (49)
dt : differential of time
ω : z component of vorticity $\boldsymbol{\omega}$

L : used in defining calculation region, for example $0 < y < L$

N : number of element

dy : length of element

y_i : midpoint of element i

α_{ij} , α_{BPj} : defined by Equation (65)

y_{BP} : boundary coordinate

R : radius of circular cylinder

(r,θ) , (ρ,ϕ) : cylindrical coordinates

R_0 : radius of virtual infinite-far boundary used in numerical calculation

(r_j,θ_i) , (r_n,θ_m) : center of element (j,i) , (n,m) or ij , mn

M , N : number of elements in circumferential and radial direction

$d\theta$, dr : equal element division in circumferential and radial directions defined by equation (84)

(x_{ij},y_{ij}) , (x_{mn},y_{mn}) : center of element defined by equation (86)

M_1 , N_1 , $d\theta_1$, dr_1 , $\theta_{1m_1n_1}$, $r_{1m_1n_1}$, $x_{1m_1n_1}$, $y_{1m_1n_1}$, … : defined by equation (94)

C_p , C_f : pressure and friction coefficients

τ : frictional stress

μ : coefficient of viscosity

D_p , D_f , D_t : pressure, friction, total drags

C_{Dp} , C_{Df} , C_{Dt} : pressure, friction, total drag coefficient

L_p , L_f , L_t : pressure, friction, total lifts

C_{Lp} , C_{Lf} , C_{Lt} : pressure, friction, total lift coefficient

$u_\infty = U$: uniform velocity

$\Delta\omega$: defined by equation (100)

$R_n = 2RU/\nu$: Reynolds number

$C_{N\theta} = Udt/(Rd\theta)$, $C_{Nr} = Udt/dr_0$: Courant number in circumferential and radial directions

dr_j : dr of element ij in case of unequal element division in radial direction

NTS : number of total time steps

C_{p_pt} : C_p obtained by potential theory

α : proportional constant of stimulus strength added on cylinder surface for certain period of time to induce rapid growth of Karman vortex

X_W : length of wake region

$Str = 2fR/U$: Strouhal number

f : frequency of Karman vortex